



Precision agricultural technology for advanced monitoring of maize yield under different fertilization and irrigation regimes: A case study in Eastern Hungary (Debrecen)

Adrienn Széles^a, László Huzsvai^b, Safwan Mohammed^{a,*}, Anikó Nyéki^c, Péter Zagyi^a, Éva Horváth^a, Károly Simon^a, Sana Arshad^d, András Tamás^a

^a Institute of Land Use, Engineering and Precision Farming Technology, Faculty of Agricultural and Food Sciences and Environmental Management, University of Debrecen, H-4032, Debrecen, Böszörményi str. 138, Hungary

^b Faculty of Economics and Business, Institute of Statistics and Methodology, University of Debrecen, H-4032, Debrecen, Böszörményi str. 138, Hungary

^c Széchenyi István University Faculty of Agricultural and Food Sciences, Department of Biosystems and Food Engineering, H-4032, Mosonmagyaróvár, Vár square 2, Hungary

^d Department of Geography, The Islamia University of Bahawalpur, Bahawalpur, 63100, Pakistan

ARTICLE INFO

Keywords:

Nitrogen treatment

Maize

Drought

Photosynthetic performance

Hungary

ABSTRACT

Precision agricultural (PrA) technology relies on the utilization of special equipment to access real time observations on plant health status, chlorophyll, nitrogen content, and soil moisture content. In this research new PrA technology (i.e., SPAD (Soil Plant Analysis Development), and UAV-based NDVI (Unmanned Aerial Vehicle-based Normalized Difference Vegetation Index) were used to monitor maize yield based on different field trials in eastern part of Hungary. Our study aimed to examine the utilization of PrA technology specifically SPAD and UAV-based NDVI measurements for monitoring maize GY under irrigated and rainfed experimental setups in Hungary with varied nitrogen treatment for the year 2022. The results showed that the SPAD increased in all treatments (14.7 %; $p < 0.05$) from V6–V8 in the rainfed treatments, decreased significantly ($p < 0.05$) by 13.9 % (R1) and 30.6 % (R3). However, implementation of irrigation significantly increased the SPAD values in majority of treatments. Also, results reveal that, under irrigated and rainfed conditions the highest UAV-based NDVI value (0.703, 0.642) was obtained in V12 (A120 treatment) and highest NDVI value (0.728, 0.662) was obtained in Vn (A120 treatment). Remarkably, irrigation led to significant differences ($p < 0.05$) of UAV-based NDVI values compared with none irrigated. On the other hand, implementation of 120 kg N ha⁻¹ before sowing led to highest GY, especially under irrigated conditions (8.649 Mg ha⁻¹). The overall mean GY under rainfed treatment was 6.256 Mg ha⁻¹, while under irrigated treatment it increased by 37.2 % and reached 8.581 Mg ha⁻¹ ($p < 0.05$). In conclusion, PrA technology will support farmers in making informed decisions regarding fertilization strategies and timing, which will in turn maximize yield and minimize risk.

1. Introduction

Maize is the second most widely grown crop globally after wheat and is a key component of animal feed playing a significant role in global agri-food systems and securing nutrition [1–3]. The global maize production accounts for 197 million ha majorly in Latin America, Asia, and Sub-Saharan Africa [2]. Europe is also reported to be a good contributor for maize in terms of increasing yield from past two decades [4] sharing 11 % of the world's maize production [2]. The three major crops i.e., wheat, maize, and rice provide 30% of the dietary calories for more than

4.5 billion people in 94 developing countries [5]. With projected world population growth, increasing demand for food products and changing diets, increasing the yield, yield stability and quality of maize is of key importance [6,7]. The situation is complicated by the loss of arable land [8] and increasingly extreme environmental conditions due to climate change [9–11]. Numerous climatic extremes including heat stress and drought conditions leads to a reduction in cereal grain filling by reducing the spikelet fertility and increasing the rate of transpiration ultimately causing a significant decline in cereal yield [12]. Frequent occurrence of droughts and high temperatures lowers the moisture

* Corresponding author.

E-mail address: safwan@agr.unideb.hu (S. Mohammed).

<https://doi.org/10.1016/j.jafr.2024.100967>

Received 15 September 2023; Received in revised form 6 November 2023; Accepted 2 January 2024

Available online 12 January 2024

2666-1543/© 2024 The Authors. Published by Elsevier B.V. This is an open access article under the CC BY-NC-ND license (<http://creativecommons.org/licenses/by-nc-nd/4.0/>).

Table 1

A review of recent studies with PrA applications in agricultural management practices.

Crops/plants	PrA tool	Objective	Main finding	Reference
Maize	UAV- multispectral and thermal sensor, SPAD	Estimate AGB of maize crop in different growth stages using PrA tools	Fusing multisource sensors data (SPAD + UAV) improved the prediction accuracy of AGB of maize	[36]
Wheat	UAV, SPAD	Estimating SPAD chlorophyll measurements from UAV multispectral indices at different nitrogen levels using machine learning	UAV multispectral indices provided accurate SPAD chlorophyll estimation using PLS regression 14 days after heading.	[37]
Rice	UAV multispectral sensor	Biomass and nitrogen estimation from UAV images	UAV indices were highly correlated with ground SPAD nitrogen measurements and better able to predict wet and dry biomass	[38]
Maize	UAV multispectral, SPAD	Predict SPAD measured chlorophyll content of maize leaves using UAV multispectral images	UAV multispectral images with machine learning algorithm effectively predicted SPAD values at different spatial scales	[39]
Wheat	Hyperspectral indices, SPAD	Predicting wheat grain yield and protein content from LAI and SPAD values at different growth stages with varying moisture and nitrogen rates	Growth monitor index with canopy spectral information provided and improved prediction of	[40]
Paddy rice	UAV multispectral	To estimate plant nitrogen content from UAV multispectral sensor, SPAD, nitrogen index	NDRE and RECI correlated with N-index.	[41]
Rice	UAV, SPAD	Estimate leaf nitrogen through UAV-derived algorithms ground truth SPAD values integrated into machine learning algorithms	UAV-algorithms provide more accurate estimation with less dependency on SPAD measurements	[42]
Ornamental plants	SPAD, GreenSeekerTM	Examine overfertilization impacts measuring plant nutrient uptake at different nitrogen levels	Small amount of controlled nitrogen monitored through non-destructive optical sensor technology proved to be effective in managing nutrient levels.	[43]
Maize	UAV multispectral, SPAD	Estimate the accuracy of SPAD from UAV-NDVI, and RENDVI under different nitrogen treatments at plot level	RENDVI camera performed better than NDVI in SPAD predictions	[44]

content, offset the maize plant growth unless provided with sufficient irrigation supported with fertilization [13]. It is expected that by 2050, there would be a 20 % decline in maize yield under projected climatic scenarios of global warming and drought stress [14].

A critical cultivation technology component of maize GY improvement is a balanced nutrient supply, with especial regard to N-supply [15, 16], as it is an essential element of plant biochemical and physiological processes [17–19]. Applying the appropriate quantity of N fertilizer can help GY growth [20], but applying excessive amounts is wasteful, increases costs [21], does not improve GY, impairs water balance, and might cause nitrate pollution [22]. Monitoring maize GY largely depends on the reliable information about maize leaf chlorophyll content during the growing season that is much needed for appropriate application of N-fertilization in plant without environmental damage [23, 24]. Chlorophyll is the photosynthetic pigment of the plant, playing a central role in light absorption, energy conversion and organic synthesis in plants [25]. Since chlorophyll content is closely related and correlated with leaf nitrogen concentration, and an important indicator for monitoring plant nitrogen status, development, growth, and GY [26]. It also provide an opportunity to schedule nitrogen fertilizer application and determine the optimal amount [27].

The use of PrA technology (refers to an information technology (IT) based farm management system) in this regard is indispensable in all types of environmental conditions [28]. PrA technology relies on the utilization of special equipment, sensor devices, real time kinematic (RTK) and un-named aerial vehicles (UAVs) to access real time observations on plant health status, chlorophyll, nitrogen, and soil moisture content [29]. Optical sensor devices like Soil Plant Analysis Development (SPAD) meter are cost effective and non-destructive handled PrA technology used to monitor in situ plant fertilization or N status to assist improving GY prediction [30]. The SPAD-502 chlorophyll meter is based on the radiation absorption in leaves in the red (R) (650 nm) and near-infrared (NIR) (940 nm) range. The 650 or red wavelength is correlated with the chlorophyll content in the leaf while 940 or NIR provides the detail of leaf moisture content and plant thickness [31]. Previously, it has been used in various studies as a PrA tool for effective farm management and GY improvement [32]. The relative chlorophyll content values at leaf level measured by the instrument are closely related to the leaf N-value and total chlorophyll concentration at different developmental stages, as confirmed by numerous researchers [16,33]. Unmanned aerial vehicle (UAV) based multispectral remote

sensing technology is more advanced PrA technology widely used to extract phenophase information, leaf area index (LAI), carotenoid estimation, and SPAD prediction [34,35]. A brief review of similar recent applications of PrA technology in different crop management practices are presented in Table 1.

The optical and thermal infrared sensors of UAVs are capable to derive several vegetation indices like normalized difference vegetation index (NDVI), normalized difference red edge index (NDRE) used to estimate the biomass, chlorophyll, and nitrogen content, and predict crop yields in high spatial resolution [44] with flexibility, rapid and non-destructive diagnosis [45,46]. It is profitable and cost-effective [47], but this can only be achieved by the optimal timing of surveys [48]. However, monitoring and measuring the plant chlorophyll and fertilization status from PrA technology largely depends on soil moisture content sourced by rainfall in natural and irrigation in human developed scenarios [40,49].

Irrigation is a key factor that influences the photosynthetic performance of maize due to severe water stress, which otherwise can greatly reduce the relative chlorophyll content and net photosynthesis, resulting in significant GY loss [50].

Formerly, studies have proven the application of SPAD and UAV PrA technology for monitoring GY under stressed and non-stressed environment [41,51,52]. For instance, a few studies reported the use of SPAD and UAV based measurements for sun-induced chlorophyll and grain yield measurements in particular experimental setup in Europe as well [53,54]. Hungary, from central Europe experienced moderate to severe drought spells in recent past years with unprecedented impacts on maize and wheat yield [55–57]. Specifically, the recent drought year of 2022 is well recognized in research [58,59] to cause agriculture drought and impact grain yield.

In this context, our study aimed to examine the utilization of PrA technology specifically SPAD and UAV-based NDVI measurements for monitoring maize GY under irrigated and rainfed experimental setups in Hungary with varied nitrogen treatment for the year 2022. Specifically, we analyzed the correlation between different levels of basal nitrogen and top-dressing treatments, irrigation, and chlorophyll content using spectral values (SPAD, UAV-based NDVI). It facilitated determining the required amount of N, the timing of its application and the influence of irrigation for achieving higher GY. Overall, the output of this research provides an effective utilization of PrA technology for grain yield monitoring proposing an optimistic future for farm management under

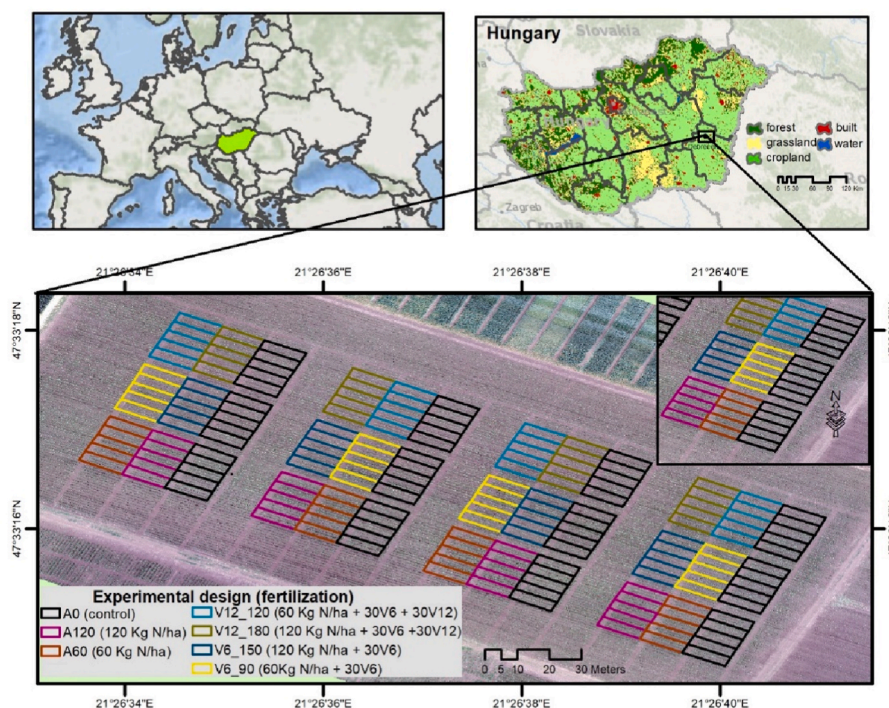


Fig. 1. Location of the experimental area. (A: Hungary, Debrecen; B: layout of the basal and top-dressing nitrogen treatment experiment, established by A. Széles, 2011).

Table 2
Nitrogen treatments and period for the factorial design.

No.	Code	Nitrogen treatments	period
1	A ₀	Control	Control
2	A ₆₀	60 kg N ha ⁻¹	Before sowing
3	A ₁₂₀	120 kg N ha ⁻¹ before sowing	Before sowing
4	V ₆ ₉₀	60 kg N ha ⁻¹ before sowing +30 kg N ha ⁻¹ during the V6 phenophase	before sowing + V6 phenophase
5	V ₆ ₁₅₀	120 kg N ha ⁻¹ before sowing +30 kg N ha ⁻¹ during the V6 phenophase	before sowing + V6 phenophase
6	V ₁₂ ₁₂₀	60 kg N ha ⁻¹ before sowing +30 kg N ha ⁻¹ during the V6 phenophase +30 kg N ha ⁻¹ during the V12 phenophase	Before sowing + V6 phenophase + V12 phenophase
7	V ₁₂ ₁₈₀	120 kg N ha ⁻¹ before sowing +30 kg N ha ⁻¹ during the V6 phenophase +30 kg N ha ⁻¹ during the V12 phenophase	Before sowing + V6 phenophase + V12 phenophase

drought and non-drought conditions to maximize the GY.

2. Materials and methods

2.1. Experimental site

This research was carried out in central Europe within the research station of the University of Debrecen (47° 33' N, 21° 26' E, altitude 111 m) (Fig. 1). The experiment was conducted using factorial design, with two-replicate. The main plots were set up with three hybrids (Merida, Armagnac, Fornad), split-plots with irrigation (rainfed, irrigated) and split-split-plots with nitrogen treatment doses.

2.2. Soil data

The soil of the experiment can be characterized with high clay loam content (42 %) with humic layer (80–100 cm), and medium-compaction, and can be classified as lowland calcareous chernozem

(Mollisol-Calcustoll or Vermustoll, USDA). The average pH_{KCl} is 6.6 and nitrogen N-supply of the soil is medium (humus content: 2.6 %, total N = 0.14–0.18 %). The soil is calcareous in the upper 80 cm, but moderately calcareous (12 %) from 100 cm. The original AL-soluble P₂O₅ content of the soil is 130 mg/kg and the AL-soluble K₂O content is 240 mg/kg.

2.3. Experimental design

Before sowing, 27 % Genesis CAN (calcium ammonium nitrate) was applied. To meet the factorial design, the nitrogen rates were split between basal and top-dressing treatments. All nitrogen doses and period are presented in Table 2.

In terms of current climate change, especially drought in Hungary, irrigation was considered as the second factor. Thus, plots were split to irrigated and none irrigated (rainfed). The total irrigation water applied was 115 mm, broken down as follows: 25 mm (21st May); 30 mm (13–16th June); 30 mm (3rd July) and 30 mm (16th July).

The maize was sown on 14.04.2022 and harvested on 05.10.2022; the plant density was 73 thousand plants/ha. The evaluation was carried out using two maize hybrids of the medium maturity group (FAO 400–499). Harvested yield GY (t ha⁻¹) was indicated by correcting it for 14 % moisture.

2.4. An outlook of climate conditions during the experiment

In the first month of the growing season (April), rainfall was in line with the average for the reference period (1981–2010) (54 mm), while temperatures were 2.2 °C lower. Rainfall in May and June was 10 mm and 19 mm respectively, only 15 and 29 % of the multiannual average (Fig. 2). This was coupled with mean temperatures in May and June that were 1 °C and 2.9 °C above the multi-year average. The drought continued in July (21 mm) and August (28 mm), and the situation was exacerbated by the fact that the monthly mean temperatures for these two months were 2.1 °C and 2.7 °C above the multi-year average. September received the highest rainfall (162 mm), more than three

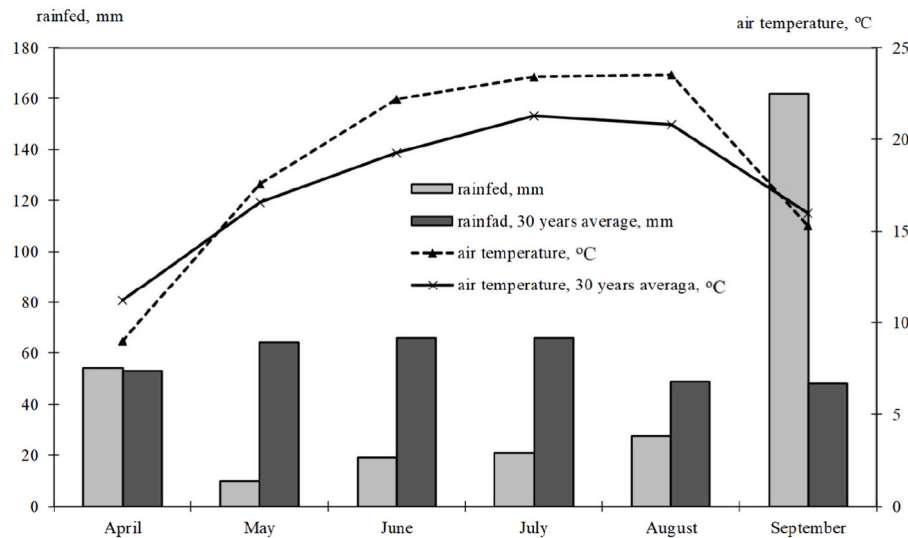


Fig. 2. Monthly amount of rainfall and average mean temperature of the growing season in 2022 and average for the period 1981–2010.

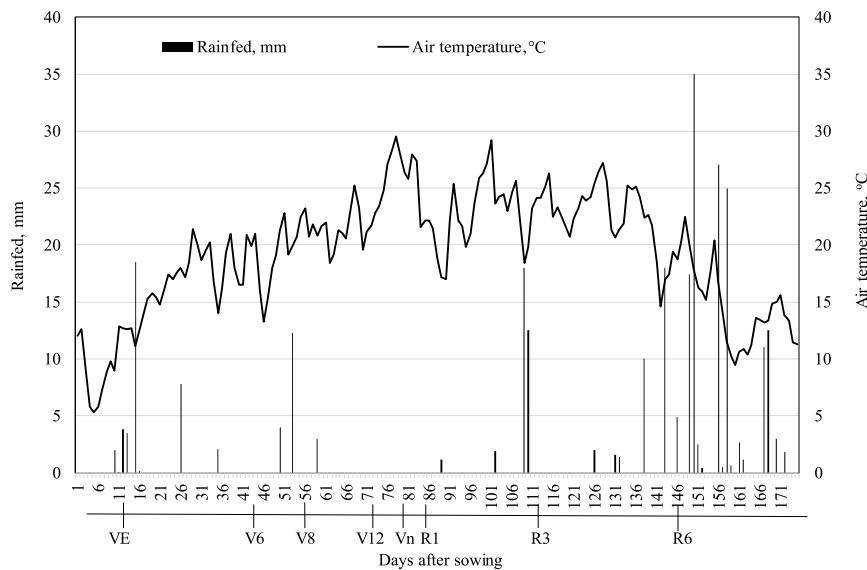


Fig. 3. Rainfall distribution and daily mean temperature trends from sowing to harvest.

times of average. (Fig. 2). Overall, the climatic conditions for the growing season 2022 (April–September) deviated from the climatic data for the reference period (1981–2010). The rainfall of the growing season was below the multi-year average (294 mm), accounting for 85 % of the average, and was characterised by an inappropriate temporal distribution. The mean temperature was 1 °C above the multi-year average (18.5 °C).

The temporal pattern of rainfall during the growing season (from sowing to harvesting) and the daily mean temperature trends are shown in Fig. 3. Of the 35 days with rainfall, 23 days were below 10 mm and 9 days were above 10 mm. Rainfall exceeding 20 mm was recorded on 3 days. Reflecting the extreme weather conditions, maize water requirements at flowering stage (R1) were 4.5–5.5 mm/ha per day, while there was only 3 mm of rainfall during the 31 days between phenophases V8 and R1, and average temperature also increased significantly (23.7 °C). Between phenophases R1-R3, there was 21 mm rainfall with an average temperature of 22.8 °C. Significant rainfall occurred after the R6 phenophase (146 mm).

Hence, Due to less rainfall and prevailing drought conditions during the growing season and the unique challenges posed by this specific climatic context, a one-year experimental duration was deemed fitting to comprehensively capture the impact of varied nitrogen treatments in rainfed and irrigated experimental setups.

2.5. PrA instruments and test methods

2.5.1. The SPAD-502

A Minolta SPAD-502 portable device (Minolta Camera Ltd., Osaka, Japan) was used for the non-destructive assessment of leaf chlorophyll content [60]. The illumination system of the device contains two photodiodes, one red (max 650 nm) and one infrared (max. 940 nm). The two photodiodes emit light alternately with equal brightness. The illuminated area is 6 mm². The two types of light pass through the leaf plate and some of it is reflected (reflection), some is absorbed (absorption) while the rest penetrates the leaf (transmission). The light that penetrates the leaf is picked up by a sensor consisting of a silicone photodiode

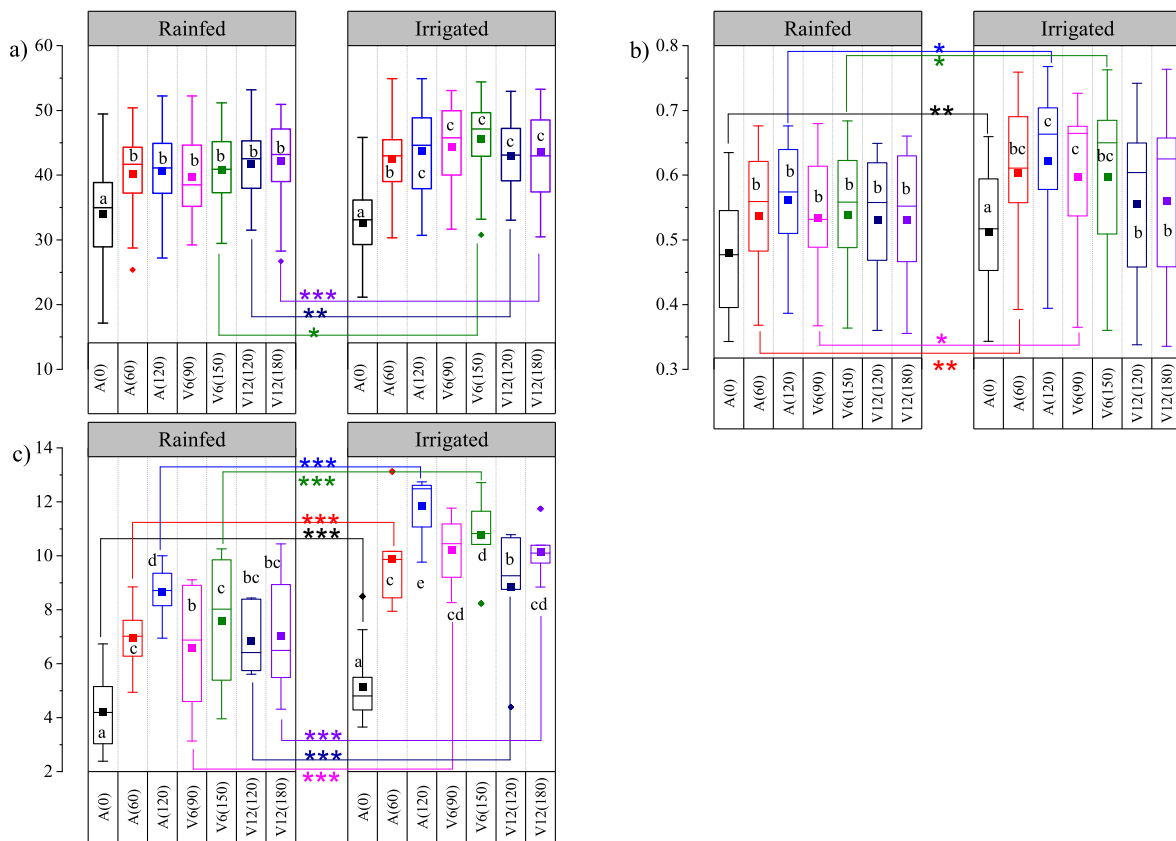


Fig. 4. Box plots of SPAD (a), UAV-based NDVI (b), and GY (c) under different treatments. (The nitrogen treatments of the values marked with different lowercase letters are significantly different from each other based on the on Duncan’s test at the $p < 0.05$ probability level. Irrigation effect: * $p < 0.5$; ** $p < 0.1$; *** $p < 0.001$).

Table 3
Effect of nitrogen treatment and irrigation on spectral values (SPAD and UAV-based NDVI) and GY of maize, 2022.

Nitrogen treatment	SPAD value	UAV-based NDVI	GY Mg ha ⁻¹
Rainfed			
A ₀	34.0a	0.479a	4.222a
A ₆₀	40.3b	0.538b	6.954bc
A ₁₂₀	40.6b	0.562b	8.649d
V ₆₉₀	39.8b	0.535b	6.586b
V ₆₁₅₀	40.8b	0.539b	7.587c
V ₁₂₁₂₀	41.1b	0.527b	6.837bc
V ₁₂₁₈₀	41.7b	0.528b	7.030bc
Average	38.5	0.518	6.256
Irrigated			
A ₀	32.6a	0.511a	5.149a
A ₆₀	42.5b	0.603bc	9.903c
A ₁₂₀	43.8bc	0.623c	11.863e
V ₆₉₀	44.4bc	0.597bc	10.220cd
V ₆₁₅₀	45.5c	0.597bc	10.782d
V ₁₂₁₂₀	43.6bc	0.561b	8.858b
V ₁₂₁₈₀	44.4bc	0.565b	10.153cd
Average	40.2	0.564	8.581
Irrigation effect			
A ₀	ns	**	***
A ₆₀	ns	**	***
A ₁₂₀	*	**	***
V ₆₉₀	**	*	***
V ₆₁₅₀	***	*	***
V ₁₂₁₂₀	ns	ns	***
V ₁₂₁₈₀	ns	ns	***
Average	**	***	***

Note: The nitrogen treatments of the values marked with different lowercase letters within the columns are significantly different from each other based on the on Duncan’s test at the $p < 0.05$ probability level. Irrigation effect: ns = not significant, * $p < 0.5$; ** $p < 0.1$; *** $p < 0.001$.

and converted into an analogue electrical signal. The instrument amplifies the electrical signal and converts it into a number. The calculation is based on the ratio of the intensity of the infrared and red light passing through the leaf. The higher the ratio, the more red light is absorbed by the leaves of the plant, which is closely related to the chlorophyll content. The SPAD value can range from 0 to over 100 [61,62]. SPAD measurements were performed in the phenological phases V6, V8, V12, Vn, R1 and R3. Measurements were taken per hybrid per Nitrogen treatment, on the 6th, 7th, and 8th plants of the second left row of each plot. Between V6 and R1 phenophase on the latest released fully developed leaf, between R1-R6 phenophase on the leaf at the ear [63].

2.5.2. UAV/drone image acquisition

The UAV-NDVI measurements were performed using a DJI Phantom 4 Pro V2 drone equipped with Sentera Double 4K TrueNDVI and TrueNDRE sensors [64] in six phenophases (V6, V8, V12, Vn, R1, R3) simultaneously with the SPAD measurements. The flying height was set to 80 m. The precise plot boundaries were determined by another PrA instrument i.e., Trimble RTK [65]. All georeferenced UAV images were stitched to make orthomosaic with a spatial resolution of 2 cm in open source WebODM program for further analysis [66]. The other products developed included digital surface model (DSM) and digital terrain model (DTM) which were not used in analysis. The orthorectified photos were further processed in open source QGIS environment for NDVI measurements.

For accurate channels (wavelengths) separation, a set of equations were used to subtract out the effect of the out of band channels [64]. These includes eq (1), 2), and 3):

$$Red = -0.966 \times DNblue + 1 \times DNred \tag{1}$$

$$NIR = 4.350 \times DNblue - 0.286 \times DNred \tag{2}$$

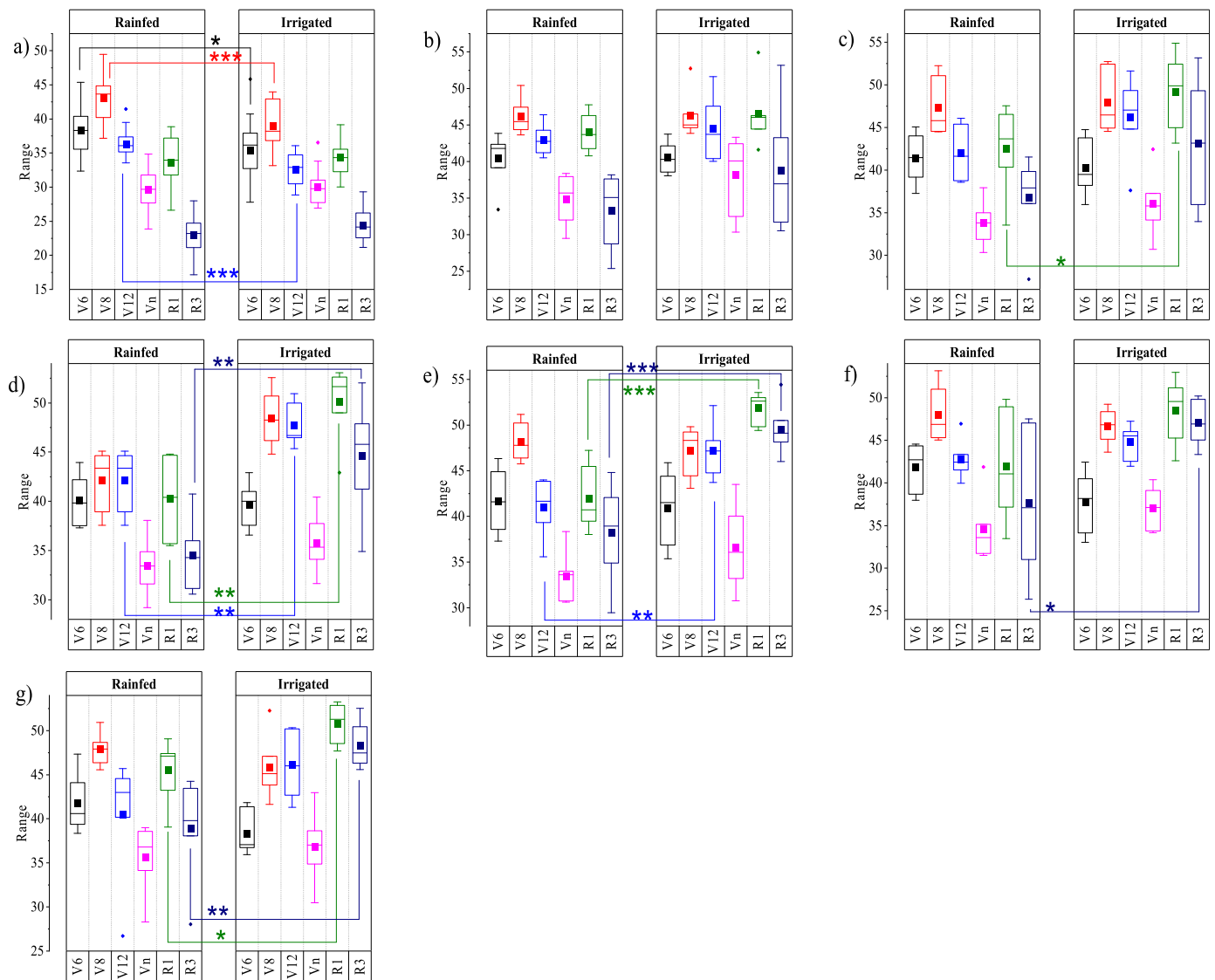


Fig. 5. Box plots of SPAD values under different nitrogen and irrigation treatments: a) A_0 , b) A_{60} , c) A_{120} , d) V_{690} , e) V_{6150} , f) V_{12120} , g) V_{12180} (Irrigation effect: * $p < 0.5$; ** $p < 0.1$; *** $p < 0.001$).

$$NDVI = \frac{NIR - RED}{NIR + RED} \quad (3)$$

The resulting NDVI images were analyzed in the QGIS environment to calculate mean NDVI of each plot using “zonal statistics” function.

2.6. Statistical analysis

First, the effects of nitrogen treatments on SPAD and UAV-NDVI for irrigated and rainfed conditions are examined in Box-plot distribution plots with significant * $p < 0.5$, ** $p < 0.1$; *** $p < 0.001$ mean difference plotting from Duncan’s test in OriginLab [67]. Multivariate factorial analysis of variance ANOVA from generalized linear model (GLM) was used to examine the effects of nitrogen treatments, irrigation, and hybrid on GY.

The comparison of mean values of different treatment practices were analyzed using Duncan multiple range test (DMRT) [68] to avoid the accumulation of first-order error. The DMRT is a post-hoc statistical analysis to examine the significant differences between various treatments of an experimental setup [69]. It significantly compares the means of all possible pairs of different treatment groups. Currently, DMRT is employed in different nitrogen treatments to evaluate the

pairwise difference in rainfed and irrigated conditions. Within the homogeneous group, the grain yields did not differ at 5 % significance level.

Furthermore, the significant relationship of nitrogen treatment with SPAD and NDVI values were examined by parabolic (quadratic) regression analysis. The independent variable was nitrogen treatment, and the dependent variables were SPAD and UAV-NDVI. The significant relationship was evaluated based on coefficient of determination (R^2). The correlation between SPAD and grain yield, and UAV-NDVI and grain yield were analyzed using bivariate linear regression analysis. The independent variables were SPAD and UAV-NDVI, and the dependent variable was grain yield. Here also, the significant relationship was evaluated based on the coefficient of determination (r^2). The statistical evaluation was performed using the latest version of the R environment and results are plotted in OriginLab.

3. Results

3.1. Effect of nitrogen treatment and irrigation on studied maize indicators

During the growing season, the SPAD values varied from 23.0 to 48.4

Table 4
Effect of nitrogen and irrigation treatments on the SPAD values of maize in phenological stages, 2022.

Nitrogen treatments	Phenological phases					
	V6	V8	V12	Vn	R1	R3
Rainfed						
A ₀	38.3a; D	43.0a; E	36.2a; D	29.7a; B	33.6a; C	23.0a; A
A ₆₀	40.4a; B	46.1a; C	43.0b; BC	34.9b; A	44.0b; BC	33.3b; A
A ₁₂₀	41.4a; B	47.3b; C	42.0b; B	33.8b; A	42.6b; B	36.7b; A
V ₆₉₀	40.1a; B	48.4b; C	42.2b; B	33.4b; A	40.3b; B	34.5b; A
V ₆₁₅₀	41.7a; B	48.2b; C	41.0b; B	33.5b; A	41.9b; B	38.2b; B
V ₁₂₁₂₀	41.8a; BC	48.0b; C	42.8b; BC	34.6b; A	41.9b; BC	37.7b; AB
V ₁₂₁₈₀	41.7a; BC	47.9b; D	40.5b; ABC	35.6b; A	45.5b; CD	38.9b; AB
Irrigated						
A ₀	35.4a; D	39.0a; E	32.6a; C	30.1a; B	34.4a; CD	24.4a; A
A ₆₀	40.5b; AB	46.3b; B	44.5b; AB	38.1b; A	46.6b; B	38.8b; A
A ₁₂₀	40.3b; AB	47.9b; C	46.2b; BC	36.0b; A	49.2bc; C	43.1bc; BC
V ₆₉₀	39.7 ab; A	48.5b; BC	47.7b; BC	35.8b; A	50.2bc; C	44.6cd; B
V ₆₁₅₀	40.9b; B	47.2b; C	47.2b; C	36.6b; A	51.8c; D	49.5d; CD
V ₁₂₁₂₀	37.7 ab; A	46.7b; B	44.8b; B	37.0b; A	48.5bc; C	47.0cd; B
V ₁₂₁₈₀	38.3 ab; A	45.8b; B	46.1b; B	36.8b; A	50.8c; C	48.3cd; BC
Irrigation effect						
A ₀	*	***	***	ns	ns	Ns
A ₆₀	ns	ns	Ns	ns	ns	Ns
A ₁₂₀	ns	ns	Ns	ns	*	Ns
V ₆₉₀	ns	ns	**	ns	**	**
V ₆₁₅₀	ns	ns	**	ns	***	***
V ₁₂₁₂₀	ns	ns	Ns	ns	ns	*
V ₁₂₁₈₀	ns	ns	Ns	ns	*	**
Average	**	*	*	ns	***	***

Note: Nitrogen treatments of mean SPAD values with different lowercase letters within columns are significantly different from each other based on the Duncan's test at $p < 0.05$ probability level. The phenophases of SPAD values with different capital letters within the row are significantly different from each other based on the Duncan's test at the $p < 0.05$ probability level. Irrigation effect: ns = not significant, * $p < 0.05$; ** $p < 0.01$; *** $p < 0.001$.

in the rainfed treatment and from 24.4 to 51.8 in the irrigated treatment. Under natural rainfall conditions, the average SPAD value was 38.5, while under irrigated conditions it was 40.2. The highest SPAD values during the whole growing season were obtained under natural rainfall conditions with treatment A₆₀ (40.3; $p < 0.05$) and under irrigated conditions with treatment V₆₁₅₀ (45.5; $p < 0.05$), which resulted in an increase of 18.5 % and 39.6 %, respectively, compared to treatment A₀ (Fig. 4, Table 3).

SPAD value increased in the V6–V8 phenophase period in the rainfed treatment but varied upon nitrogen treatment. The most significant increase (20.7 %; $p < 0.05$) was recorded in the V₆₉₀ treatment which increased the 60 kg N ha⁻¹ basal treatment (A₆₀) with an additional 30 kg N ha⁻¹ dose. After the V8 phenological phase, there was a decrease in leaf SPAD values ($p < 0.05$), 13.9 % (R1) and 30.6 % (R3) (Fig. 5d). In irrigated treatments, SPAD values increased until the V8 phenophase in treatments A₀, A₆₀ and A₁₂₀ ($p < 0.05$), whereas the top-dressing treatments (V₆₉₀, V₆₁₅₀, V₁₂₁₂₀ and V₁₂₁₈₀) increased SPAD values up to phenophase R1 ($p < 0.05$). The highest increase up to phenophase V8 was obtained with A₁₂₀ (22.8 %) and up to phenophase R1 with V₆₁₅₀ (50.6 %) (Fig. 5c and e). By the R3 phenophase, SPAD values were

identical to those measured at the V6 phenophase, averaged over the nitrogen treatments (Fig. 5a–g, Table 4). Furthermore, Duncan test revealed highly significant ($p < 0.001$) SPAD value difference in rainfed and irrigated treatment in V8 and V12 phenophase is observed in A₀ nitrogen treatment (Fig. 4a), R1 and R3 phenophase in V₆₁₅₀ nitrogen treatment (Fig. 5e).

The lowest SPAD value was detected in treatment A₀ in all phenophases, both in the rainfed and irrigated treatments. Evaluating the efficiency of the basal nitrogen and top-dressing treatments by phenophase showed that the highest value was 41.8 in phenophase V6 (V₁₂₁₂₀), but the Duncan test did not distinguish between SPAD values in different nitrogen treatments. In V8 growth stages, the highest SPAD value was measured in the A₁₂₀ treatment (47.3), an increase of 10.0 % ($p < 0.05$) compared to the A₀ treatment. After V12 phenophase until R3 phenophase, the lowest spring basal nitrogen treatment of 60 kg N ha⁻¹ (A₆₀) proved to be effective ($p < 0.05$). The nitrogen application in R3 phenophase had the greatest effect on SPAD value compared to treatment A₀ (44.8 %). The average nitrogen effect was also highest in the R3 phenophase (39.1 %). In the irrigated treatment, the statistically proven increase in the vegetative phase (V6–Vn) was obtained by the A₆₀ treatment ($p < 0.05$), while in the generative phase (R1–R3) by the A₁₂₀ treatment increased with an additional 30 kg N ha⁻¹ (V₆₁₅₀). In the vegetative stage, the V12 phenophase (36.5 %) and in the generative stage, the R3 phenophase (102.9 %) had the highest nitrogen treatment effect compared to the non-nitrogen (A₀) treatment (Table 3).

On the other hand, implementation of irrigation significantly increased the SPAD values in the majority of treatments (Table 4). For the control treatment, the irrigation has a significant impact only on the early stages V6 ($p < 0.5$), V8 ($p < 0.001$), and V12 ($p < 0.001$). While no significant impact was detected on the other stages (Table 4). For the first nitrogen level (60 kg N ha⁻¹ before sowing), the irrigation has no effects on SPAD values. However, based on the observed values, the irrigation has no effect on SPAD values in Vn stage for all nitrogen levels, where it has an impact on R1, and R3. All on all, the irrigation has a significant impact on SPAD for all phenological phases except for Vn (Table 4).

3.2. Effect of Nitrogen treatments and irrigation on the UAV-based NDVI

Nitrogen treatments and irrigation affected the UAV-based NDVI values. The values varied from 0.364 to 0.662 in the rainfed treatment and from 0.348 to 0.728 in the irrigated treatment. The overall experiment mean was 0.541. Under natural rainfall, the UAV-based NDVI for maize was 0.518, while under irrigated conditions it was 0.564. The measured data showed that the highest average value of the NDVI was obtained in A₆₀ (0.538; $p < 0.05$) in the rainfed treatments and A₁₂₀ (0.623; $p < 0.05$) in the irrigated treatments, which were 12.3 % and 21.9 % increases, respectively, compared to the treatment A₀ (Table 3).

In the rainfed treatment, maize reached the highest UAV-based NDVI value in V12 and Vn, with increases of 61.9 % and 64.8 %, respectively (Fig. 6a–g, Table 5). Then, it decreased in R1 and R3 phenophases (11.3 % and 22.3 %). The measured data showed that in V12 phenophases, the highest NDVI values ($p < 0.05$) were obtained in treatments A₀, A₆₀, V₆₉₀ and V₆₁₅₀, while in Vn phenophases, the highest values were obtained in treatments A₁₂₀, V₁₂₁₂₀ and V₁₂₁₈₀.

Also under irrigated conditions, the highest UAV-based NDVI was achieved for V12 and Vn phenophases, increasing by 72.1 % for the V12 phenophase and 77.7 % for the Vn phenophase. The values have decreased in the R1 and R3 growth phase; by 4.3 % between Vn–R1 and 17.8 % between Vn–R3. Fertilizer treatments also had an influence in this case. At the V12 phenophase, treatments A₀, V₆₉₀, V₆₁₅₀ and V₁₂₁₈₀ had a significant effect ($p < 0.05$) (Fig. 6a–d, e, & g), while the other treatments had the highest effect at the Vn phenophase (Fig. 6b,c, & f, Table 5). Overall, Duncan's test revealed a highly significant ($p < 0.001$) difference in rainfed and irrigated high NDVI values in V12 and Vn phenophase in A₆₀, A₁₂₀, and V₆₉₀ nitrogen treatments (Fig. 6b, c, & d).

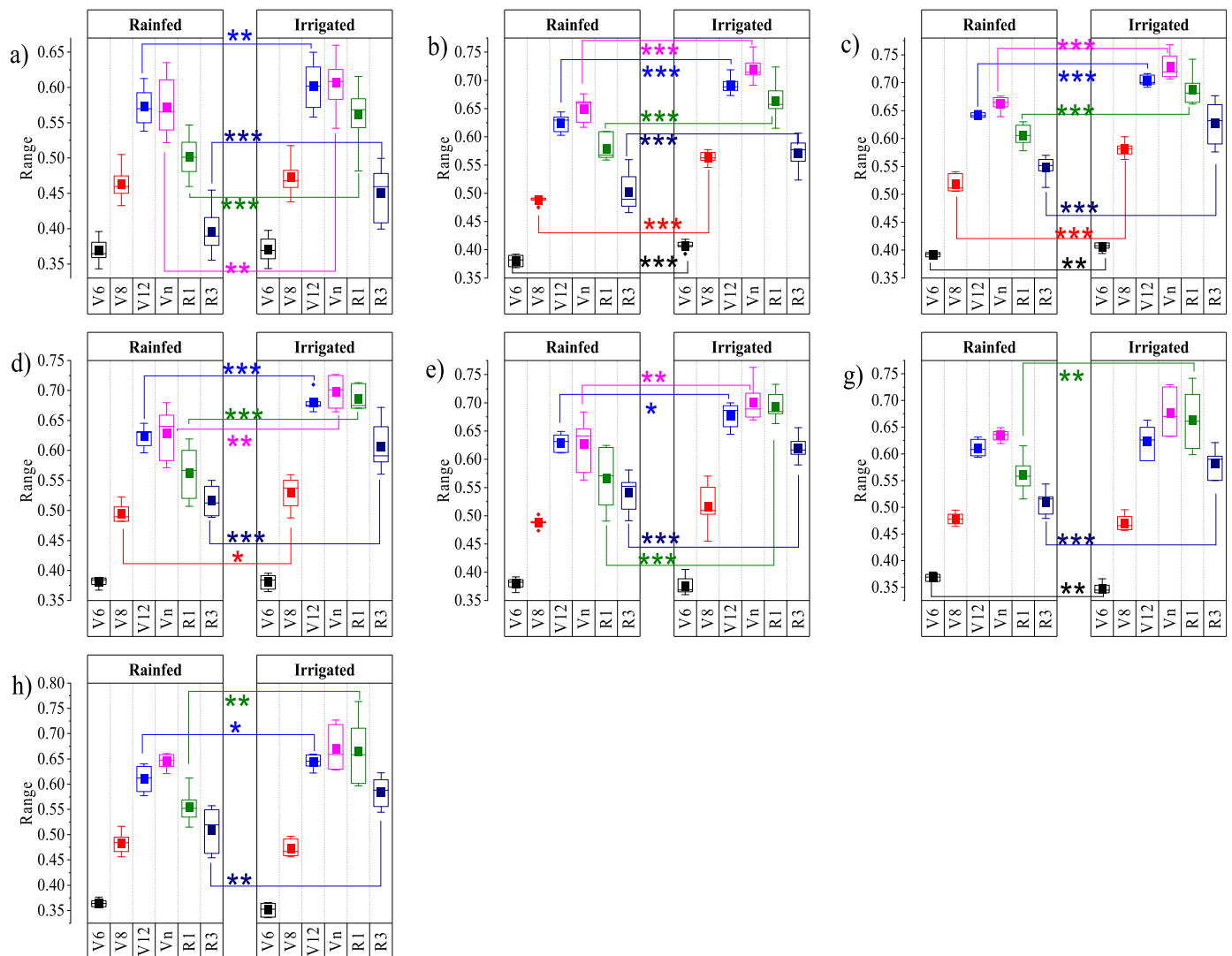


Fig. 6. Box plots of UAV-based NDVI values under different nitrogen and irrigation treatments: a) A_0 , b) A_{60} , c) A_{120} , d) V_{690} , e) V_{6150} , f) V_{12120} , g) V_{12180} (Irrigation effect: * $p < 0.05$; ** $p < 0.01$; *** $p < 0.001$).

Under natural rainfall conditions, the A_{120} treatment was proven to provide the highest UAV-based NDVI value ($p < 0.05$) throughout the vegetation period. Between treatments, the largest increase was recorded in A_{120} (38.4 %) in the R3 phenophase compared with control one. Under irrigated conditions, the result of treatment A_{60} showed the highest UAV-based NDVI value. Over all the highest UAV-based NDVI value were recorded in A_{120} (Table 5).

Similar to SPAD, the UAV-based NDVI value positively affected by irrigation. Irrigation had a positively significant effect on the average of treatments based on different phenological phases. For A_{60} and A_{120} irrigation had a distinct and substantial impact on UAV-based NDVI in all phenological phases (Table 5). Under other nitrogen treatments, the impact of irrigation on the UAV-based NDVI was inconsistent; it affected certain phenological stages while leaving others unaffected. However the average value showed that irrigation has significant impact on UAV-based NDVI under all phenological phases except for V6.

3.3. Effect of Nitrogen treatments and irrigation on grain yield

Under rainfed treatments, the A_0 provided the lowest GY (4.2 Mg ha⁻¹), which was well separated from the other treatments by Duncan's test (Table 3, Fig. 3). The 60 kg N ha⁻¹ (A_{60}) resulted in an increase of GY by 64.7 % ($p < 0.05$). This treatment did not increase GY at the 6-leaf

stage when increased with an additional 30 kg N ha⁻¹ nitrogen rate (V_{690}), and no significant increase was measured when an additional 30 kg N ha⁻¹ nitrogen rate was applied at the 12-leaf stage (V_{12120}). Treatment A_{120} provided the largest GY increase (8.649 Mg ha⁻¹), which was more than double of the GY of treatment A_0 ($p < 0.05$). However, top-dressing treatments above the basal 120 kg N ha⁻¹ resulted in a significant GY reduction ($p < 0.05$).

Under irrigated conditions, the lowest GY in terms of nitrogen (5.149 Mg ha⁻¹) was measured in the A_0 treatment. The 60 kg N ha⁻¹ (A_{60}) applied as a basal treatment resulted in a GY increase of 4.755 Mg ha⁻¹ (92.3 %; $p < 0.05$), and the 120 kg N ha⁻¹ basal treatment (A_{120}) resulted in a GY increase of 6.715 Mg ha⁻¹ (130.4 %; $p < 0.05$) compared to the A_0 treatment. Increasing the A_{60} treatment at V6 phenophase with a +30 kg N ha⁻¹ (V_{690}) resulted in a GY increase of only 3.2 %. Then, at 12-leaf stage, application of an additional 30 kg N ha⁻¹ (V_{12120}) reduced GY (-1.363, Mg ha⁻¹; $p < 0.05$). Compared to the A_{120} treatment, the effect of applying top-dressing (V_{6150}) was minimal on GY reduction. An additional 30 kg N ha⁻¹ application (V_{12180}) caused further GY reduction (-0.629 Mg ha⁻¹; $p < 0.05$). The 120 kg N ha⁻¹ basal treatment (11.863 Mg ha⁻¹) was found to have a reliable GY enhancing effect (Table 3, Fig. 3).

The main average yield was 7.419 Mg ha⁻¹ (rainfed, irrigated). The irrigated variant had a higher average yield (8.581 Mg ha⁻¹) ($p < 0.05$),

Table 5
Effect of nitrogen and irrigation on UAV-based NDVI of maize at phenological stages, 2022.

Nitrogen treatments	Phenological phases					
	V6	V8	V12	Vn	R1	R3
Rainfed						
A ₀	0.370 ab; A	0.463a; C	0.574a; E	0.572a; E	0.502a; D	0.396a; B
A ₆₀	0.381bc; A	0.488b; B	0.625b; D	0.650b; D	0.579bc; C	0.502b; B
A ₁₂₀	0.392c; A	0.519c; B	0.642c; E	0.662b; F	0.606c; D	0.548d; C
V ₆₉₀	0.381bc; A	0.495b; B	0.624bc; D	0.629b; D	0.563b; C	0.516bcd; B
V ₆₁₅₀	0.380bc; A	0.488b; B	0.630bc; D	0.627b; D	0.566b; C	0.541cd; C
V ₁₂₁₂₀	0.368 ab; A	0.478 ab; B	0.611b; E	0.635b; F	0.561b; D	0.510bc; C
V ₁₂₁₈₀	0.364a; A	0.484b; B	0.610b; D	0.645b; E	0.556b; C	0.510bc; B
Irrigated						
A ₀	0.370b; A	0.474a; C	0.602a; E	0.608a; E	0.563a; D	0.450a; B
A ₆₀	0.407c; A	0.563c; B	0.692c; D	0.720c; E	0.664b; C	0.572b; B
A ₁₂₀	0.407c; A	0.581c; B	0.703c; DE	0.728c; E	0.688b; D	0.628d; C
V ₆₉₀	0.381b; A	0.530b; B	0.680c; D	0.698bc; D	0.686b; D	0.606bcd; C
V ₆₁₅₀	0.376b; A	0.516b; B	0.678c; D	0.701bc; D	0.693b; D	0.620cd; C
V ₁₂₁₂₀	0.348a; A	0.470a; B	0.623 ab; CD	0.677b; E	0.664b; DE	0.583bc; C
V ₁₂₁₈₀	0.351a; A	0.473a; B	0.644b; D	0.670b; D	0.665b; D	0.585bc; C
Irrigation effect						
A ₀	ns	ns	**	**	***	***
A ₆₀	***	***	***	***	***	**
A ₁₂₀	**	***	***	**	***	***
V ₆₉₀	ns	*	***	**	***	***
V ₆₁₅₀	ns	ns	**	*	***	***
V ₁₂₁₂₀	**	ns	Ns	ns	**	***
V ₁₂₁₈₀	ns	ns	*	ns	**	**
Average	ns	***	***	***	***	***

Note: UAV-based NDVI values for nitrogen treatments with different lowercase letters within columns are significantly different from each other based on the Duncan's test at the $p < 0.05$ probability level. Phenophases of UAV-based NDVI values marked with different capital letters within the row are significantly different from each other based on the Duncan's test at $p < 0.05$ probability level. Irrigation effect: ns = not significant, * $p < 0.5$; ** $p < 0.1$; *** $p < 0.001$.

Table 6
Interaction between grain yield and different experimental variables from factorial ANOVA-GLM.

Source	DF	Adj SS	Adj MS	F-Value	P-Value
Model	251	4234.30	16.87	7.31	0.000
Linear	14	3916.26	279.73	121.15	0.000
Nitrogen treatment	6	2673.86	445.64	193.00	0.000
Irrigation	1	1032.89	1032.89	447.33	0.000
Hybrid	2	209.51	104.76	45.37	0.000
Phenological phases	5	0.00	0.00	0.00	1.000
2-Way Interactions	65	462.11	7.11	3.08	0.000
Nitrogen treatment *irrigation	6	184.41	30.73	13.31	0.000
Nitrogen treatment *hybrid	12	247.60	20.63	8.94	0.000
Nitrogen treatment *Phenological phases	30	0.00	0.00	0.00	1.000
irrigation*hybrid	2	30.11	15.05	6.52	0.002
irrigation*Phenological phases	5	0.00	0.00	0.00	1.000
hybrid*Phenological phases	10	0.00	0.00	0.00	1.000
3-Way Interactions	112	111.12	0.99	0.43	1.000
Nitrogen*irrigation*hybrid	12	111.12	9.26	4.01	0.000
Nitrogen*irrigation*Phenological phases	30	0.00	0.00	0.00	1.000
Nitrogen*hybrid*Phenological phases	60	0.00	0.00	0.00	1.000
irrigation*hybrid*Phenological phases	10	0.00	0.00	0.00	1.000
4-Way Interactions	60	0.00	0.00	0.00	1.000
Nitrogen*irrigation*hybrid*Phenological phases	60	0.00	0.00	0.00	1.000
Error	396	914.37	2.31		
Total	647	5148.67			

The interaction between nitrogen treatment * irrigation, nitrogen treatment * hybrid, and irrigation* hybrid had a distinct impact on GY. Interestingly, the nitrogen treatment *irrigation*hybrid interaction showed a significant impact, while the interaction between nitrogen treatment *irrigation*hybrid*Phenological phases did not show any significant impact. Overall, the fertilizer *irrigation interaction was confirmed at 0.1 % level. The results of analysis of variance showed that nitrogen application was strongly ($p < 0.001$) correlated with GY development in both rainfed and irrigated treatments.

which was 37.2 % higher than the rainfed version (6.256 Mg ha^{-1}). In all nitrogen treatments, the irrigated variants provided higher grain yields.

3.4. Interaction between yield and different experimental variables

Based on the factorial ANOVA from GLM analysis (Table 6) different factors with a significant impact on GY are identified. Table 6 showed that nitrogen treatments, irrigation, and hybrid had a significant impact

($p < 0.05$), however, the phenological phases did not exhibited any impact on GY. Analysis of variance results of chlorophyll content expressed as SPAD values in maize hybrids in rainfed and irrigated treatments showed that the main factors (nitrogen treatments and irrigation) were strongly ($p < 0.001$) correlated to the development of SPAD values (Table 6). The interaction between all variables presented in Fig. 6 revealed the highest rainfed GY (8.6 Mg ha^{-1}) with the highest NDVI (0.56) and irrigated GY (11.86 Mg ha^{-1}) with the highest NDVI

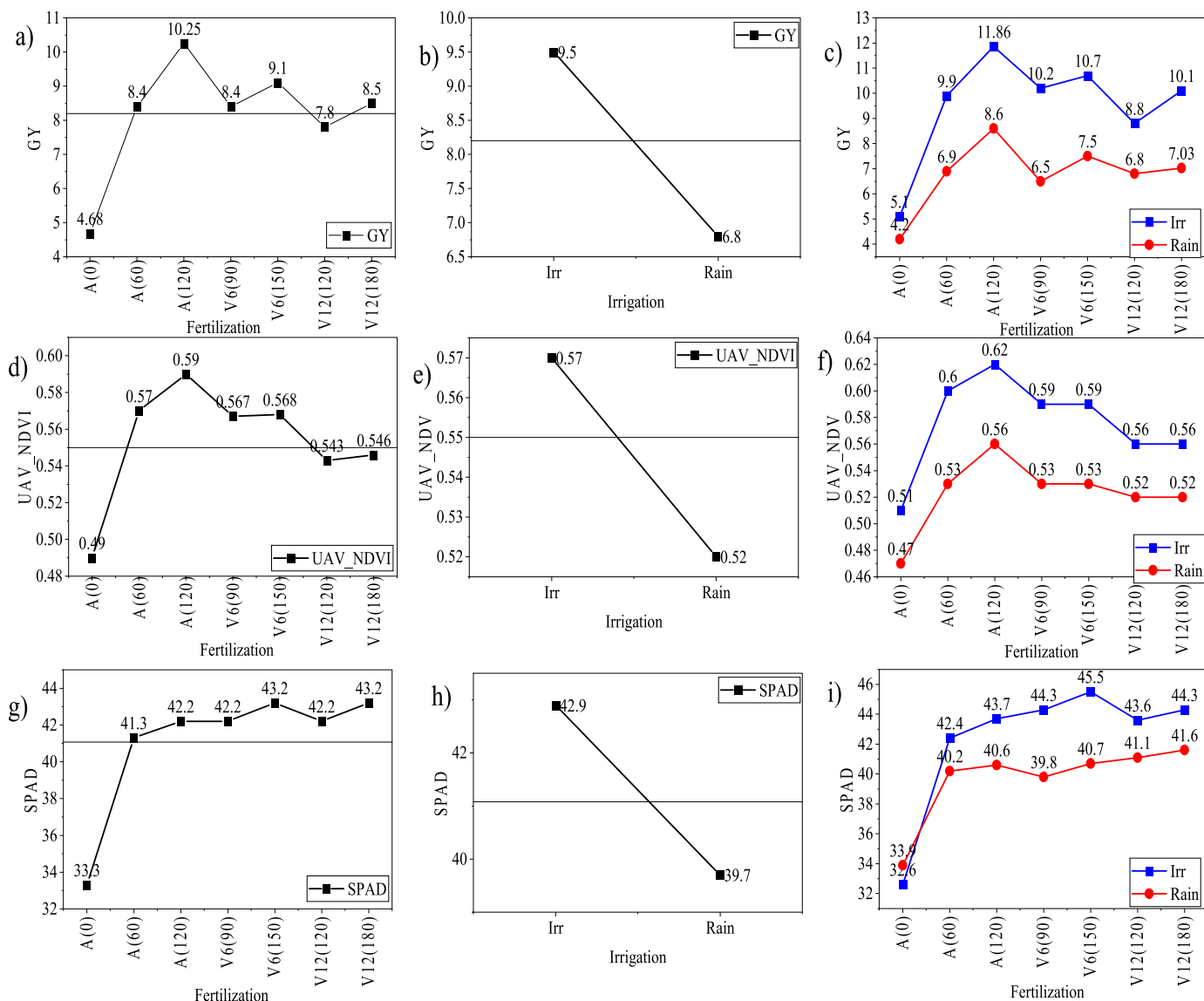


Fig. 7. Interaction between different studied variables based on the experimental data.

(0.62) was obtained under A₁₂₀ nitrogen treatment (Fig. 7c & f). The highest rainfed SPAD value (40.6) is also obtained in A₁₂₀ nitrogen treatment while highest irrigated SPAD value (45.5) is obtained in V₆₁₅₀ nitrogen treatment (Fig. 7i). The highest average SPAD value was recorded under irrigated treatment (42.9) compared with rainfed (39.7) (Fig. 7h). For GY, the irrigated average treatments exceeded the rainfed, while the best GY value were reached with A₁₂₀ treatments.

The system was mapped using observed data, as illustrated in Fig. 8. The results indicated that, irrespective of the hybrid, nitrogen level, or irrigation, early-stage measurements in V6 for both irrigated and rainfed maize resulted in low UAV-NDVI values. These values could be distinctly differentiated in Fig. 8 from the black lines.

3.5. Relationship of spectral indexes with nitrogen treatment

SPAD and UAV-based NDVI values recorded in phenophases were compared with basal nitrogen treatment and top-dressing treatments using parabolic regression-analysis (Figs. 9 and 10). The relationship between SPAD and applied amount of nitrogen showed that nitrogen application positively influenced SPAD in rainfed and irrigated treatments during the growing season. Under natural rainfall conditions, the relationship was weakly positive in the V6 phenophase ($R^2 = 0.17^{**}$)

and nitrogen treatment influenced the SPAD value in 17.0 %. The relationship between the two variables became stronger for the V8 phenophase ($R^2 = 0.4^{***}$) and further strengthened for the R1 phenophase ($R^2 = 0.47^{***}$). A stronger relationship ($R^2 = 0.67^{***}$) was observed for the R3 phenophase, with a 67 % influence of nitrogen treatment. Under irrigated conditions, similar to the rainfed treatment, the relationship was weak ($R^2 = 0.23^{**}$) for the V6 phenophase and became stronger ($R^2 = 0.83^{***}$) in R1 and R3 phenophase. Hence, in R1 and R3 developmental stages, the influence of nitrogen treatment was the most significant (83 % and 83 %) (Fig. 9).

The relationship between the UAV-based NDVI values and nitrogen application at natural rainfall was moderately close and closely correlated in the V12, R1, and R3 phenophases. The strongest correlation was observed at the R3 developmental stage ($R^2 = 0.8^{***}$). Under irrigated treatment, the parabolic relationship between the two variables was weak at the V6 phenophase and became increasingly stronger. It reached to its maximum at R3 phenophase ($R^2 = 0.82^{***}$). In this case, the differences between irrigated and rainfed treatments were lower than for SPAD (Fig. 10).

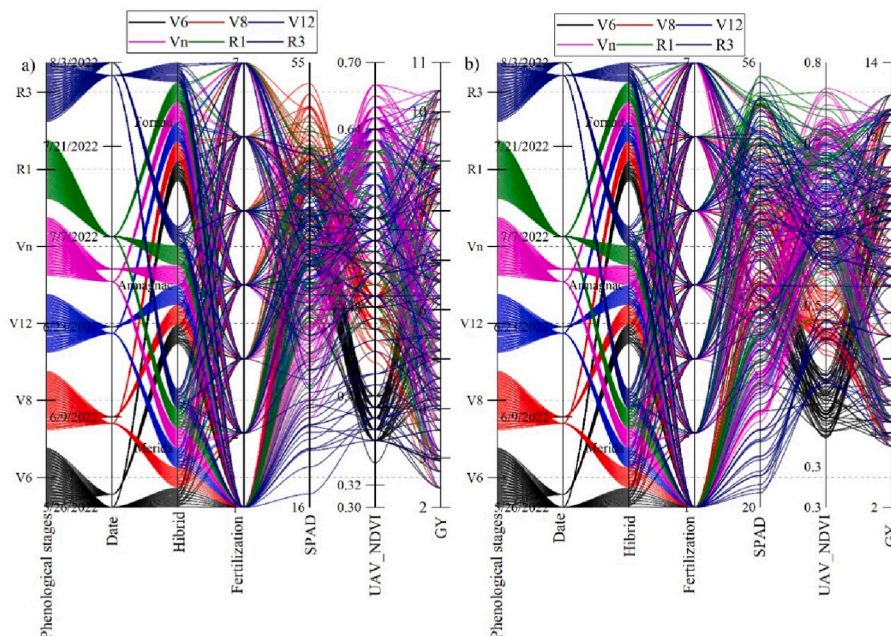


Fig. 8. System mapping, showing the interaction between different observed value of studied parameters in a) rainfed, b) irrigated.

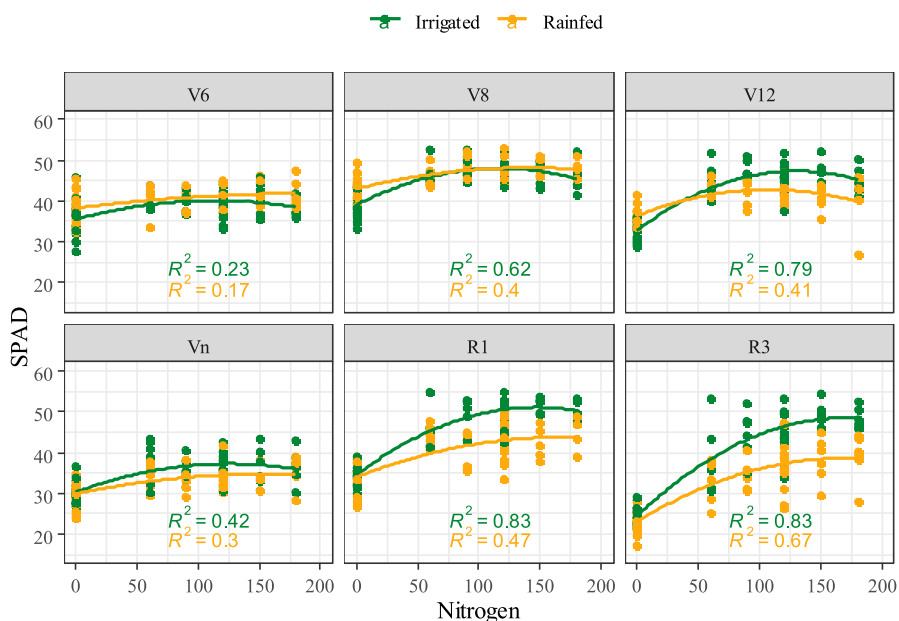


Fig. 9. A parabolic statistical relationship between N nitrogen treatment and SPAD value under rainfed and irrigated conditions, 2022.

3.6. Relationship of spectral indexes with grain yield

The significant relationship between grain yield and SPAD value under natural rainfall conditions was found to be weak to medium until silking (R1) phenophase. Furthermore, it improved to a medium level ($r^2 = 0.51^{***}$) by the R3 phenophase. For irrigated conditions, it was found to be strongest in R1 phenophase ($r^2 = 0.62^{***}$) (Fig. 11).

Furthermore, the relationship between UAV-NDVI and grain yield showed a statistically significant relationship ($r^2 = 0.7$ & 0.68^{***}) in rainfed conditions in V12 and R3 phenophase respectively. Under irrigated conditions the correlation between NDVI value and yield was medium in the V8 and V12 phenophase ($r^2 = 0.4$ – 0.52^{***}), became stronger in R1 and R3 phenophase ($r^2 = 0.62$ – 0.75^{***}) (Fig. 12).

4. Discussion

Nitrogen is a high cost but essential nutrient to gain improved maize (*Zea mays* L.) yield. Determining the amount and effective application timing of basal and top-dressing fertilizer to achieve optimal grain yields is a key research issue under drought stressed environmental conditions. To explore the issue, our research effectively utilized PrA technology including Soil Plant Analysis Development (SPAD) and Unmanned Aerial Vehicle (UAV-NDVI) measurements in a specified experimental scenario. Under current ongoing climate change, drought is considered as one of the natural hazards that has a direct impact on crop production. In this context, maize is one of the crops that is directly affected by drought and heat waves due to its origin [70]. Many studies reported the

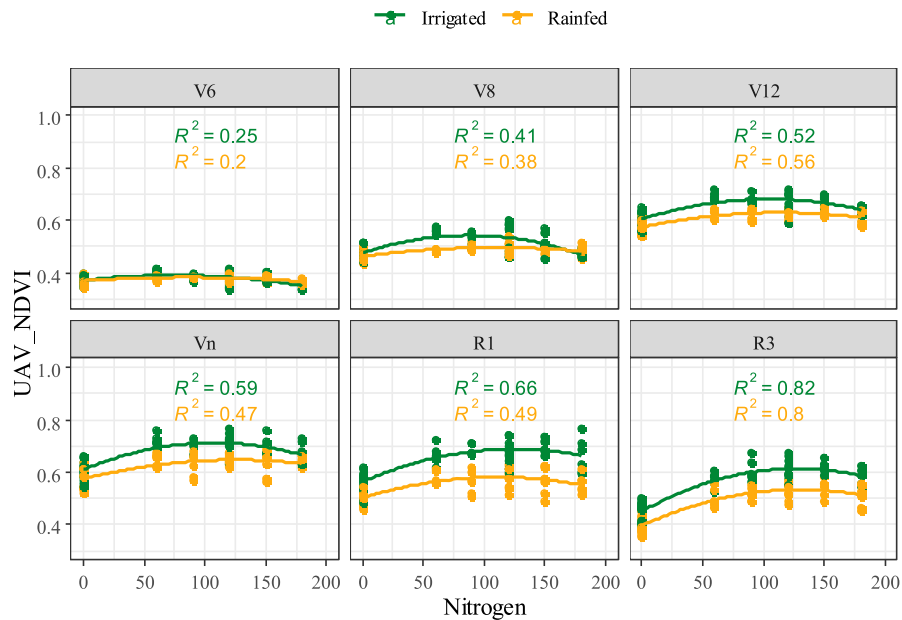


Fig. 10. Correlation between N nitrogen treatment and UAV-based NDVI under rainfed and irrigated conditions, 2022.

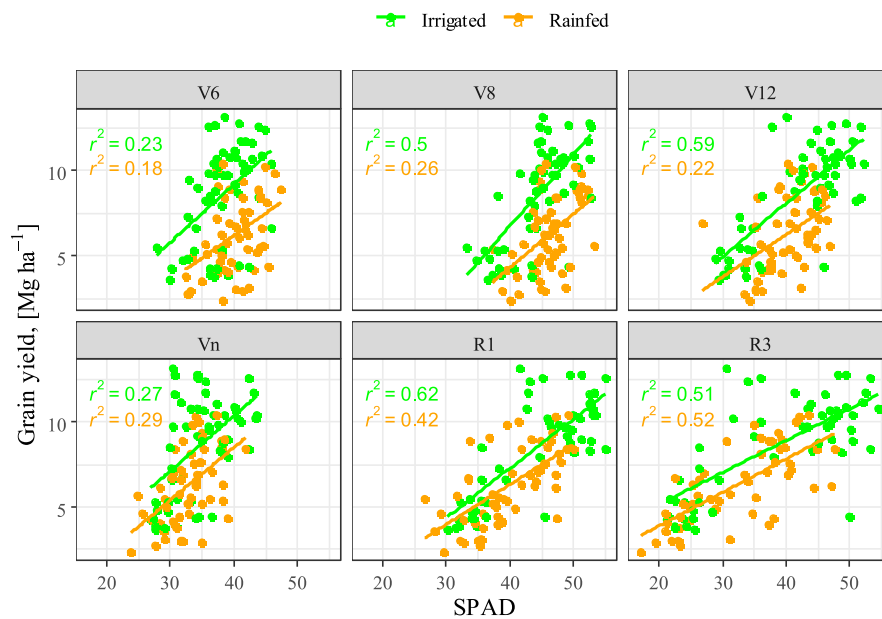


Fig. 11. Correlation between SPAD value and GY under rainfed and irrigated conditions, 2022. All correlations are significant at $p < 0.01$.

sensitivity of maize to drought [14,71]. In Hungary, Mohammed, Alsafadi [55] also reported that maize is more prone to drought events compare to wheat.

The experimental year 2022 proved to be a record-breaking for extreme weather events with significant impacts on agriculture potential of the region [72,73]. Hence meaningful PrA results are provided by our research for maize production monitoring under the rainfed and irrigated setups in the region. The major findings of the study revealed that the SPAD values are highly dependent upon the effects of N-fertilization treatments in irrigated and rainfed environments with significant high SPAD values (40.3; $p < 0.05$) reported under rainfed conditions with treatment A60 and (45.5; $p < 0.05$) under irrigated condition with treatment V6₁₅₀ (Table 3, Fig. 4). Formerly, János [74] also reported a high SPAD value under irrigated treatment compared to low SPAD in

non-irrigated treatments. Our research output also reported that 115 mm irrigated treatment did not reach on average the maximum SPAD range of 52–56 recommended by Piekielek, Fox [75]. Under rainfed conditions, the early top-dressing (V6) suggested by Jaynes [76] had its effect and there was a significant ($p < 0.05$) increase for all nutrient levels for the V8 phenophase. Furthermore, in agreement with other research findings [77,78], Following V8 phenophase, water deficit significantly ($p < 0.05$) reduced SPAD, which did not contribute to greater accumulation of pre-R1 dry matter. Furthermore, V12 and R3 phenophases had the highest effects of fertilizers compared to (A0) treatment. Phenophase analysis further revealed that under irrigated conditions in V12 phenophase, maize leaves had higher SPAD values than in the rainfed treatment (Table 4, Fig. 5). Due to irrigation and top-dressing treatments applied at V6 and V12 phenophases, the highest

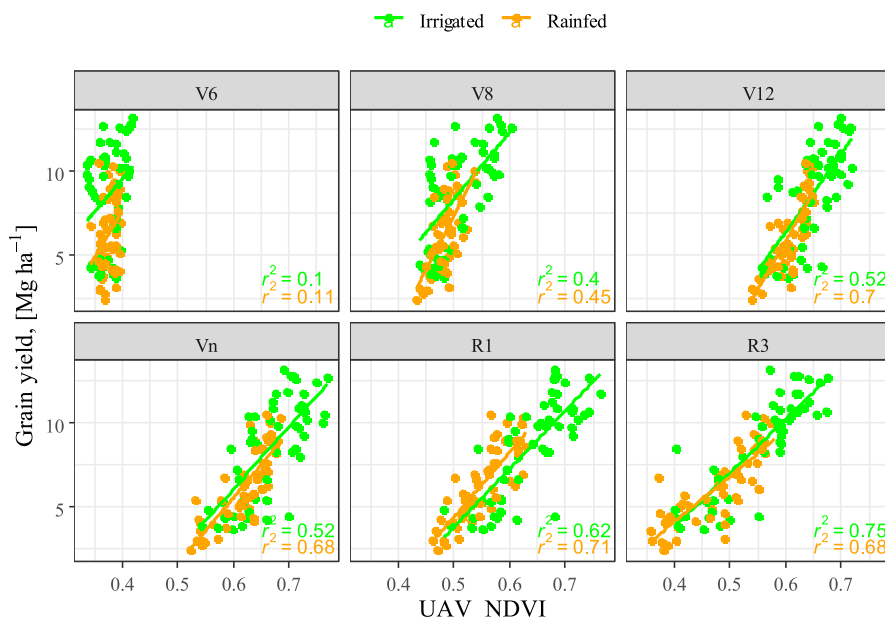


Fig. 12. UAV-based NDVI and GY correlation under rainfed and irrigated conditions. All correlations are significant at $p < 0.01$.

SPAD value developed at silking (R1) stage, the highest increase was observed with the V6₁₅₀ treatment.

Like SPAD, the UAV-based NDVI values averaged low i.e., 0.518 in the rainfed treatment and high i.e., 0.564 in the irrigated treatment, with a significant difference between the two treatments ($p < 0.001$) as also reported by Zhang, Han [79]. Significantly ($p < 0.05$) highest UAV-based NDVI values over the entire growing season in rainfed and irrigated treatments were detected in V12 and Vn phenophase with treatment A₁₂₀ and proved to be most effective for achieving high GY (Table 5, Fig. 6). The correlation analysis of GY and UAV-NDVI spectral values in agreement with [80] revealed that the early growth stages (V6 and V8) show a weaker correlation with GY while (V12 and Vn) showed a strong correlation with GY.

Further research findings exposed that due to extreme weather anomalies in 2022, top-dressing had no GY enhancement reflecting the findings of Venterea and Coulter [81], as the water stress reduced the transpiration of plants causing a decline in N uptake [33,82]. For instance Ref. [57], also reported that several precipitation characteristics including onset and cessation dates, and rainy days frequency tend to impact the maize yield in different climatic scenarios in Hungary. Another recent study by Rawat, Sharda [83] suggested the significant role of climate (in terms of severe heat and less rain) for maize yield predictions. Moreover, the negative impact of high temperature is also reported by Liu, Yu [84] reducing the chlorophyll index and net photosynthetic rate shortening the kernel filling duration. Recent historical climatic conditions of the EU substantially impacted the maize yield in rainfed and irrigated conditions with varying fertilization treatments [85]. Currently, our findings revealed that the highest grain yields were obtained with the application of the spring basal treatment (A₁₂₀), that is in agreement with the results of Drury, Reynolds [86] in both the rainfed and irrigated treatments. Moreover, significant ($p < 0.001$) irrigation effects were detected at all nutrient levels with the most significant effect in the V6₁₂₀ treatment compared to the A₀ treatment.

Overall, the coefficient of determination R^2 of N-nitrogen treatment with both SPAD and NDVI are significantly ($p < 0.001$) strong in irrigated condition compared to rainfed condition except for phenophase 6 where they have weak correlation (Figs. 9 and 10). Hence, SPAD and NDVI are more recommendable to predict maize GY under irrigated condition. From these results, the sequence of SPAD correlation with

maize GY based on R^2 in irrigated conditions is as: R1 (0.62) > V12 (0.59) > R3 (0.51) > V8 (0.5) > Vn (0.27) > V6 (0.23) and the sequence of NDVI with maize GY is as: R3 > (0.75) > R1 (0.62) > Vn, V12 (0.52) > V8 (0.4) > V6 (0.1) (Figs. 11 and 12). Overall, the results of the correlation between SPAD and NDVI spectral values and GY agree with other research findings [87,88]. Hence, we can conclude that spectral response at regenerative phenophase (R1 and R3) are recommendable for GY estimation [80,89].

Our research provides a meaningful analysis of PrA technology for effective farm management under irrigated and rainfed conditions in drought or stressed environmental condition, however, the results of study could be more comparable by using other UAV indices as used in other studies [90–92].

5. Conclusions

In the last few decades, the agricultural sector has experienced significant advancements by integration of advanced agricultural research and technology. Among them, PrA is one of the new technologies that are involved in agricultural production. PrA is one of the supporting tools that help to improve agricultural production and monitor plant health to achieve the maximum yield. In this research, SPAD and UAV-based NDVI were used to monitor maize growth in Hungary. The output of this research can be summarized as follow:

- 1 Different fertilization levels in different maize growing stage led to significant differences ($p < 0.05$) in SPAD, UAV-based NDVI, and GY between rainfed and irrigated treatments.
- 2 Irrigation had increased the yield of maize significantly ($p < 0.05$) in all treatments.
- 3 SPAD increased in all treatments in the V6–V8 phenophase period under rainfed conditions. However, implementation of irrigation significantly increased the SPAD values in the majority of treatments.
- 4 Under irrigated and rainfed conditions the highest UAV-based NDVI value (0.703, 0.642) was obtained in V12 (A₁₂₀ treatment) and highest NDVI value (0.728, 0.662) was obtained in Vn (A₁₂₀ treatment), thus it is recommended to use UAV-based NDVI in these stages.
- 5 Irrigation led to significant differences ($p < 0.05$) of UAV-based NDVI values compared with none irrigated.

- 6 Based on the output of this research, implementation of 120 kg N ha⁻¹ before sowing led to highest GY, especially under irrigated conditions (8.649 Mg ha⁻¹). On the other hand, both Fertilization*irrigation had a positive significant impact on GY.
- 7 The highest correlation was obtained between fertilization and UAV-based NDVI ($r = 0.8$) under irrigated conditions in R3 maize growing stage. A similar pattern emerged where the highest correlation between UAV-based NDVI and GY was obtained in R3, also under irrigated conditions.

Overall, this research recommends using irrigation with 120 kg N ha⁻¹ before sowing to increase the maize yield, however more research is needed to confirm this recommendation. Also, monitoring the crop using PrA, could indicate potential yield. In this sense, high correlation between UAV-based NDVI in R3 stages could reflect high SPAD value and potential high yield.

Declaration of competing interest

The authors declare that they have no known competing financial interests or personal relationships that could have appeared to influence the work reported in this paper.

Data availability

Data will be made available on request.

Acknowledgments

the research behind the study was carried out in the scope of the TKP2021-NKTA-32 project, funded by the National Research Development and Innovation Fund, under the TKP2021-NKTA call for proposals. Also, this paper was supported by the János Bolyai Research Scholarship of the Hungarian Academy of Sciences.

References

- [1] P. Ranum, J.P. Peña-Rosas, M.N. Garcia-Casal, Global maize production, utilization, and consumption, *Ann. N. Y. Acad. Sci.* 1312 (1) (2014) 105–112, <https://doi.org/10.1111/nyas.12396>.
- [2] O. Erenstein, M. Jaleta, K. Sonder, K. Mottaleb, B.M. Prasanna, Global maize production, consumption and trade: trends and R&D implications, *Food Secur.* 14 (5) (2022) 1295–1319, <https://doi.org/10.1007/s12571-022-01288-7>.
- [3] U. Grote, A. Fasse, T.T. Nguyen, O. Erenstein, Food security and the dynamics of wheat and maize value chains in Africa and Asia, *Front. Sustain. Food Syst.* 4 (2021), <https://doi.org/10.3389/fsufs.2020.617009>.
- [4] D.K. Ray, N.D. Mueller, P.C. West, J.A. Foley, Yield trends are insufficient to double global crop production by 2050, *PLoS One* 8 (6) (2013) e66428, <https://doi.org/10.1371/journal.pone.0066428>.
- [5] B. Shiferaw, B.M. Prasanna, J. Hellin, M. Bänziger, Crops that feed the world 6. Past successes and future challenges to the role played by maize in global food security, *Food Secur.* 3 (3) (2011) 307–327, <https://doi.org/10.1007/s12571-011-0140-5>.
- [6] D. Fróna, J. Szenderák, M. Harangi-Rákos, The challenge of feeding the world, *Sustainability* 11 (20) (2019) 5816, <https://www.mdpi.com/2071-1050/11/20/5816>.
- [7] D. Neupane, P. Adhikari, D. Bhattarai, B. Rana, Z. Ahmed, U. Sharma, D. Adhikari, Does climate change affect the yield of the top three cereals and food security in the world? *Earth* 3 (1) (2022) 45–71, <https://www.mdpi.com/2673-4834/3/1/4>.
- [8] W.F. Laurance, J. Sayer, K.G. Cassman, Agricultural expansion and its impacts on tropical nature, *Trends Ecol. Evol.* 29 (2) (2014) 107–116, <https://doi.org/10.1016/j.tree.2013.12.001>.
- [9] D.B. Lobell, W. Schlenker, J. Costa-Roberts, Climate trends and global crop production since 1980, *Science* 333 (6042) (2011) 616–620, <https://doi.org/10.1126/science.1204531>.
- [10] M. Gammans, P. Mérel, A. Ortiz-Bobea, Negative impacts of climate change on cereal yields: statistical evidence from France, *Environ. Res. Lett.* 12 (5) (2017) 054007, <https://doi.org/10.1088/1748-9326/aa6b0c>.
- [11] M.A. Waqas, X. Wang, S.A. Zafar, M.A. Noor, H.A. Hussain, M. Azher Nawaz, M. Farooq, Thermal stresses in maize: effects and management strategies, *Plants* 10 (2) (2021) 293, <https://www.mdpi.com/2223-7747/10/2/293>.
- [12] M. Tigchelaar, D.S. Battisti, R.L. Naylor, D.K. Ray, Future warming increases probability of globally synchronized maize production shocks, *Proc. Natl. Acad. Sci. USA* 115 (26) (2018) 6644–6649, <https://doi.org/10.1073/pnas.1718031115>.
- [13] B.M. Prasanna, J.E. Cairns, P.H. Zaidi, Y. Beyene, D. Makumbi, M. Gowda, C. Magorokosho, M. Zaman-Allah, M. Olsen, A. Das, M. Worku, J. Gethi, B.S. Vivek, S.K. Nair, Z. Rashid, M.T. Vinayam, A.B. Issa, F. San Vicente, T. Dhlwipao, X. Zhang, Beat the stress: breeding for climate resilience in maize for the tropical rainfed environments, *Theor. Appl. Genet.* 134 (6) (2021) 1729–1752, <https://doi.org/10.1007/s00122-021-03773-7>.
- [14] H. Webber, F. Ewert, J.E. Olesen, C. Müller, S. Fronzek, A.C. Ruane, M. Bourgault, P. Martre, B. Ababaei, M. Bindi, R. Ferrise, R. Finger, N. Fodor, C. Gabaldón-Leal, T. Gaiser, M. Jabloun, K.-C. Kersebaum, J.I. Lizaso, I.J. Lorite, L. Manceau, M. Moriondo, C. Nendel, A. Rodríguez, M. Ruiz-Ramos, M.A. Semenov, S. Siebert, T. Stella, P. Stratonovitch, G. Trombi, D. Wallach, Diverging importance of drought stress for maize and winter wheat in Europe, *Nat. Commun.* 9 (1) (2018) 4249, <https://doi.org/10.1038/s41467-018-06525-2>.
- [15] F.A. Sucunza, F.H. Gutiérrez Boem, F.O. García, M. Boxler, G. Rubio, Long-term phosphorus fertilization of wheat, soybean and maize on Mollisols: soil test trends, critical levels and balances, *Eur. J. Agron.* 96 (2018) 87–95, <https://doi.org/10.1016/j.eja.2018.03.004>.
- [16] A. Rhezali, A.E. Aissaoui, Feasibility study of using absolute SPAD values for standardized evaluation of corn nitrogen status, *Nitrogen* 2 (3) (2021) 298–307, <https://www.mdpi.com/2504-3129/2/3/20>.
- [17] S.J. Leghari, N.A. Wahocho, G.M. Laghari, A. HafeezLaghari, G. MustafaBhabhan, K. HussainTalpur, T.A. Bhutto, S.A. Wahocho, A.A. Lashari, Role of nitrogen for plant growth and development: a review, *Adv. Environ. Biol.* 10 (2016) 209+, <https://link.gale.com/apps/doc/A472372583/AONE?u=anon-330e2b66&id=googleScholar&xid=fe94c25f>.
- [18] V. Szilvia, Z. László, J. Csaba, Regulation effect of different water supply to the nitrogen and carbon metabolism, in: O. Alexandre Bosco de (Ed.), *Abiotic and Biotic Stress in Plants*, IntechOpen: Rijeka, 2019. Ch. 9.
- [19] M. Anas, F. Liao, K.K. Verma, M.A. Sarwar, A. Mahmood, Z.-L. Chen, Q. Li, X.-P. Zeng, Y. Liu, Y.-R. Li, Fate of nitrogen in agriculture and environment: agronomic, eco-physiological and molecular approaches to improve nitrogen use efficiency, *Biol. Res.* 53 (1) (2020) 47, <https://doi.org/10.1186/s40659-020-00312-4>.
- [20] C. Bojtor, Á. Illés, S.M. Nasir Mousavi, A. Széles, B. Tóth, J. Nagy, C.L. Marton, Evaluation of the nutrient composition of maize in different NPK fertilizer levels based on multivariate method analysis, *Int. J. Agron.* 2021 (2021) 5537549, <https://doi.org/10.1155/2021/5537549>.
- [21] A. Széles, K. Kovács, S. Ferencsik, The effect of crop years and nitrogen basal and top dressing on the yield of different maize genotypes and marginal revenue, *Időjárás/Quarterly Journal of The Hungarian Meteorological Service* 123 (3) (2019) 265–278.
- [22] M. Nazir, R. Pandey, T.O. Siddiqi, M.M. Ibrahim, M.I. Qureshi, G. Abraham, K. Vengavasi, A. Ahmad, Nitrogen-deficiency stress induces protein expression differentially in low-N tolerant and low-N sensitive maize genotypes, *Front. Plant Sci.* 7 (2016), <https://doi.org/10.3389/fpls.2016.00298>.
- [23] F. Tei, S. Nicola, P. Benincasa, *Advances in Research on Fertilization Management of Vegetable Crops*, vol. 1, Springer, 2017.
- [24] R. Gaj, P. Szulc, I. Siatkowski, H. Waligóra, Assessment of the effect of the mineral fertilization system on the nutritional status of maize plants and grain yield prediction, *Agriculture* 10 (9) (2020), <https://doi.org/10.3390/agriculture10090404>.
- [25] S. Hörteneister, B. Krätzler, Chlorophyll breakdown in higher plants, *Biochim. Biophys. Acta Bioenerg.* 1807 (8) (2011) 977–988, <https://doi.org/10.1016/j.bbabi.2010.12.007>.
- [26] B. Ghimire, D. Timsina, J. Nepal, Analysis of chlorophyll content and its correlation with yield attributing traits on early varieties of maize (*Zea mays* L.), *J. Maize Res. Dev.* 1 (1) (2015) 134–145.
- [27] H. Yang, J.P. Yang, F.H. Li, N. Liu, Replacing the nitrogen nutrition index by SPAD values and analysis of effect factors for estimating rice nitrogen status, *Agron. J.* 110 (2) (2018) 545–554, <https://doi.org/10.2134/agnonj2017.09.0532>.
- [28] D.M.K.S. Hemathilake, D.M.C.C. Gunathilake, Chapter 32 - high-productive agricultural technologies to fulfill future food demands: hydroponics, aquaponics, and precision/smart agriculture, in: R. Bhat (Ed.), *Future Foods*, Academic Press, 2022, pp. 555–567.
- [29] N. Zhang, M. Wang, N. Wang, Precision agriculture—a worldwide overview, *Comput. Electron. Agric.* 36 (2) (2002) 113–132, [https://doi.org/10.1016/S0168-1699\(02\)00096-0](https://doi.org/10.1016/S0168-1699(02)00096-0).
- [30] A.A. Khoddamzadeh, B.L. Dunn, Application of optical sensors for nitrogen management in Chrysanthemum, *Hortscience* 51 (7) (2016) 915–920, <https://doi.org/10.21273/HORTSCI.51.7.915>.
- [31] T.M. Blackmer, J.S. Schepers, Use of a chlorophyll meter to monitor nitrogen status and schedule fertigation for corn, *J. Prod. Agric.* 8 (1) (1995) 56–60, <https://doi.org/10.2134/jpa1995.0056>.
- [32] H.-I. Zheng, Y.-c. Liu, Y.-I. Qin, Y. Chen, M.-s. Fan, Establishing dynamic thresholds for potato nitrogen status diagnosis with the SPAD chlorophyll meter, *J. Integr. Agric.* 14 (1) (2015) 190–195, [https://doi.org/10.1016/S2095-3119\(14\)60925-4](https://doi.org/10.1016/S2095-3119(14)60925-4).
- [33] A.V. Széles, A. Megyes, J. Nagy, Irrigation and nitrogen effects on the leaf chlorophyll content and grain yield of maize in different crop years, *Agric. Water Manag.* 107 (2012) 133–144, <https://doi.org/10.1016/j.agwat.2012.02.001>.
- [34] P.J. Zarco-Tejada, M.V. González-Dugo, E. Fereres, Seasonal stability of chlorophyll fluorescence quantified from airborne hyperspectral imagery as an indicator of net photosynthesis in the context of precision agriculture, *Rem. Sens. Environ.* 179 (2016) 89–103, <https://doi.org/10.1016/j.rse.2016.03.024>.
- [35] K. Liu, Q.-b. Zhou, W.-b. Wu, T. Xia, H.-j. Tang, Estimating the crop leaf area index using hyperspectral remote sensing, *J. Integr. Agric.* 15 (2) (2016) 475–491, [https://doi.org/10.1016/S2095-3119\(15\)61073-5](https://doi.org/10.1016/S2095-3119(15)61073-5).

- [36] W. Zhai, C. Li, S. Fei, Y. Liu, F. Ding, Q. Cheng, Z. Chen, CatBoost algorithm for estimating maize above-ground biomass using unmanned aerial vehicle-based multi-source sensor data and SPAD values, *Comput. Electron. Agric.* 214 (2023) 108306, <https://doi.org/10.1016/j.compag.2023.108306>.
- [37] Q. Wu, Y. Zhang, Z. Zhao, M. Xie, D. Hou, Estimation of relative chlorophyll content in spring wheat based on multi-temporal UAV remote sensing, *Agronomy* 13 (1) (2023) 211, <https://www.mdpi.com/2073-4395/13/1/211>.
- [38] A.F. Duque, D. Patino, J.D. Colorado, E. Petro, M.C. Rebollo, I.F. Mondragon, N. Espinosa, N. Amézquita, O.D. Puentes, D. Méndez, A. Jaramillo-Botero, Characterization of rice yield based on biomass and SPAD-based leaf nitrogen for large genotype plots, *Sensors* 23 (13) (2023) 5917, <https://www.mdpi.com/1424-8220/23/13/5917>.
- [39] J. Ji, N. Li, H. Cui, Y. Li, X. Zhao, H. Zhang, H. Ma, Study on monitoring SPAD values for multispatial spatial vertical scales of summer maize based on UAV multispectral remote sensing, *Agriculture* 13 (5) (2023) 1004, <https://www.mdpi.com/2077-0472/13/5/1004>.
- [40] S. Liu, Z. Hu, J. Han, Y. Li, T. Zhou, Predicting grain yield and protein content of winter wheat at different growth stages by hyperspectral data integrated with growth monitor index, *Comput. Electron. Agric.* 200 (2022) 107235, <https://doi.org/10.1016/j.compag.2022.107235>.
- [41] Y.-P. Wang, Y.-C. Chang, Y. Shen, Estimation of nitrogen status of paddy rice at vegetative phase using unmanned aerial vehicle based multispectral imagery, *Precis. Agric.* 23 (1) (2022) 1–17, <https://doi.org/10.1007/s11119-021-09823-w>.
- [42] J.D. Colorado, N. Cera-Bornacelli, J.S. Caldas, E. Petro, M.C. Rebollo, D. Cuellar, F. Calderon, I.F. Mondragon, A. Jaramillo-Botero, Estimation of nitrogen in rice crops from UAV-captured images, *Rem. Sens.* 12 (20) (2020) 3396, <https://www.mdpi.com/2072-4292/12/20/3396>.
- [43] A. Freidenreich, G. Barraza, K. Jayachandran, A.A. Khoddamzadeh, Precision agriculture application for sustainable nitrogen management of Justicia brandegeana using optical sensor technology, *Agriculture* 9 (5) (2019) 98, <https://www.mdpi.com/2077-0472/9/5/98>.
- [44] L. Deng, Z. Mao, X. Li, Z. Hu, F. Duan, Y. Yan, UAV-based multispectral remote sensing for precision agriculture: a comparison between different cameras, *ISPRS J. Photogrammetry Remote Sens.* 146 (2018) 124–136, <https://doi.org/10.1016/j.isprsjprs.2018.09.008>.
- [45] D.C. Tsouros, S. Bibi, P.G. Sarigiannidis, A review on UAV-based applications for precision agriculture, *Information* 10 (11) (2019) 349, <https://www.mdpi.com/2078-2489/10/11/349>.
- [46] P. Nevavuori, N. Narra, P. Linna, T. Lipping, Crop yield prediction using multitemporal UAV data and spatio-temporal deep learning models, *Rem. Sens.* 12 (23) (2020) 4000, <https://www.mdpi.com/2072-4292/12/23/4000>.
- [47] E.E. da Silva, F.H. Rojo Baio, L.P. Ribeiro Teodoro, C.A. da Silva Junior, R. S. Borges, P.E. Teodoro, UAV-multispectral and vegetation indices in soybean grain yield prediction based on in situ observation, *Remote Sens. Appl.: Society and Environment* 18 (2020) 100318, <https://doi.org/10.1016/j.rsase.2020.100318>.
- [48] M. Latella, F. Sola, C. Camporeale, A density-based algorithm for the detection of individual trees from LiDAR data, *Rem. Sens.* 13 (2) (2021) 322, <https://www.mdpi.com/2072-4292/13/2/322>.
- [49] S. Irmak, R. Sandhu, M.S. Kukul, Multi-model projections of trade-offs between irrigated and rainfed maize yields under changing climate and future emission scenarios, *Agric. Water Manag.* 261 (2022) 107344, <https://doi.org/10.1016/j.agwat.2021.107344>.
- [50] G. Li, B. Zhao, S. Dong, J. Zhang, P. Liu, W. Lu, Controlled-release urea combining with optimal irrigation improved grain yield, nitrogen uptake, and growth of maize, *Agric. Water Manag.* 227 (2020) 105834, <https://doi.org/10.1016/j.agwat.2019.105834>.
- [51] J. Jiang, K. Johansen, C.S. Stanschewski, G. Wellman, M.A.A. Mousa, G.M. Fiene, K.A. Asiry, M. Tester, M.F. McCabe, Phenotyping a diversity panel of quinoa using UAV-retrieved leaf area index, SPAD-based chlorophyll and a random forest approach, *Precis. Agric.* 23 (3) (2022) 961–983, <https://doi.org/10.1007/s11119-021-09870-3>.
- [52] A.D. Boursianis, M.S. Papadopoulou, P. Diamantoulakis, A. Liopa-Tsakalidi, P. Barouchas, G. Salahas, G. Karagiannidis, S. Wan, S.K. Goudos, Internet of things (IoT) and agricultural unmanned aerial vehicles (UAVs) in smart farming: a comprehensive review, *Internet of Things* 18 (2022) 100187, <https://doi.org/10.1016/j.iot.2020.100187>.
- [53] N. Wang, B. Siegmund, U. Rascher, J.G.P.W. Clevers, O. Muller, H. Bartholomeus, J. Bendig, D. Masiliunas, R. Pude, L. Kooistra, Comparison of a UAV- and an airborne-based system to acquire far-red sun-induced chlorophyll fluorescence measurements over structurally different crops, *Agric. For. Meteorol.* 323 (2022) 109081, <https://doi.org/10.1016/j.agrformet.2022.109081>.
- [54] M. Le Bail, M.-H. Jeuffroy, C. Bouchard, A. Barbotin, Is it possible to forecast the grain quality and yield of different varieties of winter wheat from Minolta SPAD meter measurements? *Eur. J. Agron.* 23 (4) (2005) 379–391, <https://doi.org/10.1016/j.eja.2005.02.003>.
- [55] S. Mohammed, K. Alsafadi, G.O. Enaruvbe, B. Bashir, A. Elbeltagi, A. Széles, A. Alsalmán, E. Harsányi, Assessing the impacts of agricultural drought (SPI/SPEI) on maize and wheat yields across Hungary, *Sci. Rep.* 12 (1) (2022) 8838, <https://doi.org/10.1038/s41598-022-12799-w>.
- [56] V. Potopová, T. Trifan, M. Trnka, C. De Michele, D. Semerádová, M. Fischer, J. Meitner, M. Musiolková, N. Muntean, B. Clothier, Copulas modelling of maize yield losses – drought compound events using the multiple remote sensing indices over the Danube River Basin, *Agric. Water Manag.* 280 (2023) 108217, <https://doi.org/10.1016/j.agwat.2023.108217>.
- [57] E. Harsányi, B. Bashir, S. Arshad, A. Ocwa, A. Vad, A. Alsalmán, I. Bácskai, T. Rátonyi, O. Hijazi, A. Széles, S. Mohammed, Data mining and machine learning algorithms for optimizing maize yield forecasting in central Europe, *Agronomy* 13 (5) (2023) 1297, <https://www.mdpi.com/2073-4395/13/5/1297>.
- [58] K. Biró, E. Kovács, Agro-climatic Analysis for Agricultural Adaptation in Hungary, *Periodica Polytechnica Social and Management Sciences*, 2023, <https://doi.org/10.3311/PPso.22482>.
- [59] L. Báder, J. Szilágyi, Widening gap of land evaporation to reference evapotranspiration implies increasing vulnerability to droughts in Hungary, *Period. Polytech. Civ. Eng.* 67 (4) (2023) 1028–1037, <https://doi.org/10.3311/PPci.21836>.
- [60] J. Uddling, J. Gelang-Alfredsson, K. Piikki, H. Pleijel, Evaluating the relationship between leaf chlorophyll concentration and SPAD-502 chlorophyll meter readings, *Photosynth. Res.* 91 (1) (2007) 37–46, <https://doi.org/10.1007/s11120-006-9077-5>.
- [61] Chlorophyll Meter SPAD-502 Instruction Manual, Konica Minolta Sensing, Inc., Plainfield, IL, USA, 1989.
- [62] X.M. Connelly, The Use of a chlorophyll meter (SPAD-502) for field determinations of red mangrove (*Rhizophora mangle* L.) leaf chlorophyll amount, *NASA University Research Centers Technical Advances in Education, Aeronautics, Space, Autonomy, Earth and Environment 1* (URC97032) (1997).
- [63] C. Costa, L.M. Dwyer, P. Dutilleul, D.W. Stewart, B.L. Ma, D.L. Smith, Inter-relationships of applied nitrogen, spad, and yield of leafy and non-leafy maize genotypes, *J. Plant Nutr.* 24 (8) (2001) 1173–1194, <https://doi.org/10.1081/PLN-100106974>.
- [64] J. Csajbók, E. Buday-Bódi, A. Nagy, Z.Z. Fehér, A. Tamás, I.C. Virág, C. Bojtor, F. Forgács, A.M. Vad, E. Kutasy, Multispectral analysis of small plots based on field and remote sensing surveys—a comparative evaluation, *Sustainability* 14 (6) (2022) 3339, <https://www.mdpi.com/2071-1050/14/6/3339>.
- [65] A. Stoll, H. Dieter Kutzbach, Guidance of a forage harvester with GPS, *Precis. Agric.* 2 (3) (2000) 281–291, <https://doi.org/10.1023/A:1011842907397>.
- [66] G. Vacca, WEB open drone map (WebODM) a software open source to photogrammetry process, in: *Fig Working Week 2020, Smart surveyors for land and water management*, 2020.
- [67] J.G. Moberly, M.T. Bernards, K.V. Waynant, Key features and updates for origin 2018, *J. Cheminf.* 10 (2018) 1–2.
- [68] R.J. Tallarida, R.B. Murray, Duncan multiple range test, in: R.J. Tallarida, R. B. Murray (Eds.), *Manual of Pharmacologic Calculations: with Computer Programs*, Springer New York, New York, NY, 1987, pp. 125–127.
- [69] S.K. Meena, B.S. Dwivedi, M.C. Meena, S.P. Datta, V.K. Singh, R.P. Mishra, D. Chakraborty, A. Dey, V.S. Meena, Effect of nutrient management on soil carbon quantities, qualities, and stock under rice-wheat production system, *Agriculture* 12 (11) (2022) 1822, <https://www.mdpi.com/2077-0472/12/11/1822>.
- [70] D.B. Lobell, M.J. Roberts, W. Schlenker, N. Braun, B.B. Little, R.M. Rejesus, G. L. Hammer, Greater sensitivity to drought accompanies maize yield increase in the U.S. Midwest, *Science* 344 (6183) (2014) 516–519, <https://doi.org/10.1126/science.1251423>.
- [71] S. Daryanto, L. Wang, P.-A. Jacinthe, Global synthesis of drought effects on maize and wheat production, *PLoS One* 11 (5) (2016) e0156362, <https://doi.org/10.1371/journal.pone.0156362>.
- [72] A. Buzási, Comparative assessment of heatwave vulnerability factors for the districts of Budapest, Hungary, *Urban Clim.* 42 (2022) 101127, <https://doi.org/10.1016/j.ueclim.2022.101127>.
- [73] K. Biró, E. Kovács, Impact of the 2022 Drought Shock on the Adaptive Capacity of Hungarian Agriculture, 2023, <https://doi.org/10.3311/ppso.22482>.
- [74] N. János, Impact of fertilization and irrigation on the correlation between the soil plant analysis development value and yield of maize, *Commun. Soil Sci. Plant Anal.* 41 (11) (2010) 1293–1305, <https://doi.org/10.1080/00103621003759304>.
- [75] W.P. Piekielek, R.H. Fox, J.D. Toth, K.E. Macneal, Use of a chlorophyll meter at the early dent stage of corn to evaluate nitrogen sufficiency, *Agron. J.* 87 (3) (1995) 403–408, <https://doi.org/10.2134/agonj1995.00021962008700030003x>.
- [76] D.B. Jaynes, Nitrate loss in subsurface drainage and corn yield as affected by timing of sidedress nitrogen, *Agric. Water Manag.* 130 (2013) 52–60, <https://doi.org/10.1016/j.agwat.2013.08.010>.
- [77] R.E. Brevedan, D.B. Egli, Short periods of water stress during seed filling, leaf senescence, and yield of soybean, *Crop Sci.* 43 (6) (2003) 2083–2088, <https://doi.org/10.2135/cropsci2003.2083>.
- [78] L. Wang, B. Ren, B. Zhao, P. Liu, J. Zhang, Comparative yield and photosynthetic characteristics of two corn (*Zea mays* L.) hybrids differing in maturity under different irrigation treatments, *Agriculture* 12 (3) (2022) 365, <https://www.mdpi.com/2077-0472/12/3/365>.
- [79] Y. Zhang, W. Han, X. Niu, G. Li, Maize crop coefficient estimated from UAV-measured multispectral vegetation indices, *Sensors* 19 (23) (2019) 5250, <https://www.mdpi.com/1424-8220/19/23/5250>.
- [80] B. Yang, W. Zhu, E.E. Rezaei, J. Li, Z. Sun, J. Zhang, The optimal phenological phase of maize for yield prediction with high-frequency UAV remote sensing, *Rem. Sens.* 14 (7) (2022) 1559, <https://www.mdpi.com/2072-4292/14/7/1559>.
- [81] R.T. Venterea, J.A. Coulter, Split application of urea does not decrease and may increase nitrous oxide emissions in rainfed corn, *Agron. J.* 107 (1) (2015) 337–348, <https://doi.org/10.2134/agonj14.0411>.
- [82] D.R. Bista, S.A. Heckathorn, D.M. Jayawardena, S. Mishra, J.K. Boldt, Effects of drought on nutrient uptake and the levels of nutrient-uptake proteins in roots of drought-sensitive and -tolerant grasses, *Plants* 7 (2) (2018) 28, <https://www.mdpi.com/2223-7747/7/2/28>.
- [83] M. Rawat, V. Sharda, X. Lin, K. Roozeboom, Climate change impacts on rainfed maize yields in Kansas: statistical vs. Process-based models, *Agronomy* 13 (10) (2023) 2571, <https://www.mdpi.com/2073-4395/13/10/2571>.

- [84] X. Liu, Y. Yu, S. Huang, C. Xu, X. Wang, J. Gao, Q. Meng, P. Wang, The impact of drought and heat stress at flowering on maize kernel filling: insights from the field and laboratory, *Agric. For. Meteorol.* 312 (2022) 108733, <https://doi.org/10.1016/j.agrformet.2021.108733>.
- [85] M.S. Lopes, Will temperature and rainfall changes prevent yield progress in Europe? *Food Energy Secur.* 11 (2) (2022) e372, <https://doi.org/10.1002/fes3.372>.
- [86] C.F. Drury, W.D. Reynolds, X.M. Yang, N.B. McLaughlin, T.W. Welacky, W. Calder, C.A. Grant, Nitrogen source, application time, and tillage effects on soil nitrous oxide emissions and corn grain yields, *Soil Sci. Soc. Am. J.* 76 (4) (2012) 1268–1279, <https://doi.org/10.2136/sssaj2011.0249>.
- [87] L. Zhang, Y. Niu, H. Zhang, W. Han, G. Li, J. Tang, X. Peng, Maize canopy temperature extracted from UAV thermal and RGB imagery and its application in water stress monitoring, *Front. Plant Sci.* 10 (2019) 1270, <https://doi.org/10.3389/fpls.2019.01270>.
- [88] R. Fieuzal, C. Marais Sicre, F. Baup, Estimation of corn yield using multi-temporal optical and radar satellite data and artificial neural networks, *Int. J. Appl. Earth Obs. Geoinf.* 57 (2017) 14–23, <https://doi.org/10.1016/j.jag.2016.12.011>.
- [89] T. Spitzkó, Z. Nagy, Z. Zsubori, C. Szóke, T. Berzy, J. Pintér, C. Marton, Connection between normalized difference vegetation index and yield in maize, *Plant Soil Environ.* 62 (7) (2016) 293–298, <https://doi.org/10.17221/676/2015-PSE>.
- [90] A. Elazab, R.A. Ordóñez, R. Savin, G.A. Slafer, J.L. Araus, Detecting interactive effects of N fertilization and heat stress on maize productivity by remote sensing techniques, *Eur. J. Agron.* 73 (2016) 11–24, <https://doi.org/10.1016/j.eja.2015.11.010>.
- [91] L. Qiao, W. Tang, D. Gao, R. Zhao, L. An, M. Li, H. Sun, D. Song, UAV-based chlorophyll content estimation by evaluating vegetation index responses under different crop coverages, *Comput. Electron. Agric.* 196 (2022) 106775, <https://doi.org/10.1016/j.compag.2022.106775>.
- [92] W. Zhu, E.E. Rezaei, H. Nouri, Z. Sun, J. Li, D. Yu, S. Siebert, UAV-based indicators of crop growth are robust for distinct water and nutrient management but vary between crop development phases, *Field Crops Res.* 284 (2022) 108582, <https://doi.org/10.1016/j.fcr.2022.108582>.